

Chapter 6

Forensic Comparison of Soil Samples

Jisook Min, Kiwook Kim, Sangcheol Heo, and Yurim Jang

Abstract As a preliminary experiment to test the discriminating ability of forensic soil analysis techniques and obtain area-specific information, soil samples were collected from eight areas near the eastern branch of the National Forensic Service (NFS) located in Gangwondo, an eastern province of South Korea. The soil samples were collected from five spots within each sample area using a small-scale (1 m²) soil sampling technique; for each of these five spots, two samples were collected from two places in each spot, (i) one from the surface and (ii) another from 30 cm below the surface. For each sample, the color of the sample with particle size in the range 53–500 μm and the major constituents were determined using a spectrophotometer and X-ray fluorescence spectrometer (XRF), respectively. The carbon content and carbon isotope ratio of the part of the sample of particle size below 53 μm were measured using an element analyzer-isotope ratio mass spectrometer (EA-IRMS). The canonical discriminant and XRF analyses showed an excellent color discriminating ability of 87.5% and 88.8%, respectively, with respect to the major constituents. The EA-IRMS results showed that the soils obtained from a 30-cm depth below the surface were generally more enriched in δ¹³C (0/00) than the surface soils, and that the surface soils contained a higher carbon amount (%). The canonical discriminant analysis confirmed 100% discriminating ability when all three soil characteristics (i.e., color, composition, and content) were used in the analysis. Out of the two functions obtained from the analysis, Function 1 exhibited greater potential for explaining the SiO₂, Fe₂O₃, and TiO₂; thus, Area 6 and 7 could be more easily differentiated than the other areas using this function. Function 2 exhibited greater potential for explaining color factor b* (δ¹³C and C content), and could more efficiently differentiate Area 2 and 5. However, different results were obtained within the same area based on the soil depth. Therefore, when performing a comparative sampling analysis in forensic science, due care should be taken to prevent the mixing of adjacent soils from various depths. Better results can be achieved by collecting soil samples from different spots within the same area.

J. Min (✉) • K. Kim • S. Heo • Y. Jang

National Forensic Service, 331-1 Shinwol7-Dong Yangcheon-Gu, 158-707 Seoul, Korea

e-mail: minjs@korea.kr

© Springer International Publishing Switzerland 2016

H. Kars, L. van den Eijkel (eds.), *Soil in Criminal and Environmental Forensics*,
Soil Forensics, DOI 10.1007/978-3-319-33115-7_6

71

6.1 Introduction

Soil samples are most frequently used in forensic investigations associated with a wide variety of criminal acts and incidences such as abandonment of corpse, rape, robbery, and traffic accidents. The most frequently encountered difficulties in soil analyses are the extreme complexity of soil composition and minuscule sample volume. Moreover, apart from the identification of comparing samples, it is often required to obtain the area-specific soil information of a given type of soil. However, because of the lack of systematically developed techniques, such area-specific information data obtained from existing techniques do not meet the actual information needs. To improve this situation, there is an urgent need for establishing measurement techniques that are capable of analyzing minuscule samples and studying area-specific features using the state-of-the-art equipment (Junger 1996). In this study, the discriminating abilities of various soil-analysis methods were tested using various techniques, and the results of area-specific information obtained was reviewed.

Some of the forensic soil analysis methods are as follows: mineral morphology and particle state analysis (Graves 1979), hydrometer-assisted mineral morphological analysis (Chaperlin and Howarth 1983), color inspection (Guedes et al. 2011), size and classification inspection, and pollen analysis. The comparative analysis of biotic components found in soil can be performed, among others, using chromatography, Fourier transform infrared (FT-IR) spectroscopy, and Raman spectroscopy (Wheals and Noble 1972; Reuland and Trinler 1981; Cox et al. 2000; Thanasoulis et al. 2002). The investigation methods for comparative analyses of the ratio of rare-earth elements to major mineral constituents, using XRF (Fitton 1997) and X-ray diffraction (XRD), inductively-coupled plasma (ICP), and laser ablation inductively-coupled plasma mass spectrometry (LA-ICP-MS), have also been reported (Petraco et al. 2000; Bull et al. 2006; Pye et al. 2007; Petraco et al. 2008; Pye and Blott 2009; Murray 2012). Furthermore, the most recent addition to this list of techniques is the determination of carbon and nitrogen contents and isotope ratios (Meyers 1994; Pye et al. 2006).

When different soils are compared, one of the most important discriminating factors is color. Color differences are the results of different compositions of biotic and abiotic materials in soil. They provide cumulative information such as the original place of the soils, decomposition residues of native plants and animals in that place, and other organic matters such as excrementitious matters. In many cases, the surface of a soil particle consists of iron, aluminum, organic matter, clay, and other substances, and gives important information on the history of the soil sample. Brown, yellow, or red color of the soil indicates a high concentration of iron oxides in the soil. Brown color soils predominate in warm and humid weather conditions, yellow color soils predominate in water environment, and soils turn grey when their iron content migrates to groundwater or other water sources.

Red color soils indicate high temperature or oxidizing conditions existing in soil, and the red color of soil becomes stronger not only as the iron content increases, but also as the oxidation advances. The iron components in soils exist in the forms of hematite, limonite, goethite, lepidocrocite, etc. The black mineral tone of soil is generally associated with the presence of manganese or iron-manganese composites. The color of soils is also influenced by biotic matters irrespective of the presence of abiotic matters. The organic materials on soil surface usually appear black. The humus infiltrated into mineral soil layers is dark in color, and the soil with iron and humic acid has a dark blackish red-brown color. Although such information based on the color of soil can be used as a primary discriminating factor in forensic soil comparison, given the fact that the data would be presented in a criminal court, it is important to perform scientifically the color investigation using a spectrophotometer instead of a rough visual examination.

In particular, when the soil evidences have similar colors, more sophisticated forensic analysis techniques are required. In such cases, besides morphological investigation using a spectrophotometer and stereo microscope, high-precision analyses should be performed, such as elemental analysis using a XRF, comparison of carbon contents and carbon isotope ratios using an EA-IRMS, and mineral identification using a XRD.

Therefore, the soil samples were collected from eight areas in Wonju, (Gangwondo, South Korea) and the following analyses were performed: color inspection using a spectrophotometer, elemental analysis using a XRF, and measurement of carbon content and carbon isotope ratio using an EA-IRMS. With the help of these quantitative analyses, the discriminating abilities of various techniques used for soil identification were evaluated, and their abilities to obtain area-specific information were ascertained. Furthermore, statistical analyses of the abovementioned samples were conducted using SPSS 18.0 and soft independent modeling of class analogy (SIMCA).

6.2 Materials and Methods

6.2.1 Area Description and Sample Collection

The soil samples were collected from eight areas (Fig. 6.1 and Table 6.1) in Wonju (Gangwondo, South Korea) for this study. The soil sampling was carried out on five spots in each of the areas as follows: a center point (c) and four corner points (a, b, d, and e) of a square (Fig. 6.2).

From each spot, the soil samples were collected from the surface (S) and 30-cm depth (D) below the surface, and then dried for at least 5 days in a well-ventilated shady place. To ensure the homogeneity of the dried samples, they were separated using 500 and 53- μm -mesh sieves.



Fig. 6.1 Locations of the eight soil sampling areas

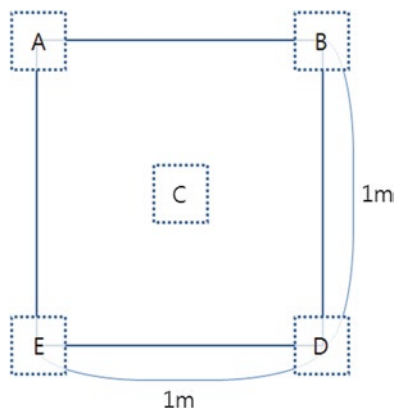
Table 6.1 Soil sampling plots and their locations

Area	Location
1area	Empty lot in the NFS eastern branch
2area	Near Moonmak Industrial Complex
3area	Under a river bridge
4area	Residential area near streets
5area	Fishing zone near a dam
6area	Roadside pasturage near factories
7area	River beach sands
8area	Soil near the river

6.2.2 Color Determination of Soils Using Spectrophotometer

The particles in soils are classified into coarse sand, medium sand, fine sand, silt, and clay in decreasing order of size. As the size decreases, red or red-brown color becomes increasingly apparent, while as the size increases, grey and yellow colors become more and more dominant. Therefore, sieves were used to separate the soils in specific sizes (53–500 μm) prior to determining their color using a

Fig. 6.2 Soil sampling areas



spectrophotometer (Spectrophotometer CM-5, Konika Minolta, Japan), which can measure the wavelength range between 360 and 740 nm. Before using the spectrophotometer, a black-and-white color calibration was carried out, and each sample was measured for five times. The results of color measurement were expressed according to the CIE L^* , a^* , b^* (CIELAB) color space.

6.2.3 Elemental Analysis of Soils Using X-ray Fluorescence Spectrometer

Beads were made from the soils ranging from 53 to 500 μm and subjected to an XRF analysis for determining the contents of major elements. Using K2 Prime (Katanax, Canada), beads of 30-mm diameter were fabricated from the soil dough mixed at the ratio of soil:flux (lithium tetraborate):remover (lithium bromide)=0.5 g:4.5 g:0.03 g. The SiO_2 , Al_2O_3 , Fe_2O_3 , K_2O , CaO , and TiO_2 contents were analyzed using an XRF spectrometer (M4 Tornado, Bruker, Germany). Each sample was measured for five times.

6.2.4 Carbon Isotope Ratio and Carbon Content of Soils Using EA-IRMS

In this measurement, samples smaller than 53 μm were used. They were wrapped in tin capsules after the weight check, and their $\delta^{13}\text{C}$ (0/00) and carbon contents (%) were measured using CH-6 and urea as the reference standards. Each sample was measured in triplicates. Our attempt to perform measurements for nitrogen isotope ratio and carbon content was aborted because $\delta^{15}\text{N}$ could not be measured even with as much as 20 mg sample. Given the usual forensic settings in which the sample

analyses should be often performed with relatively small amounts of sample, the nitrogen-related measurements are considered inadequate. The elemental analyses were performed using an elemental analyzer (Euro EA 3000, Euro Vector, Italy), and Isoprime (GV instrument, UK) was used as the mass spectrometer. The degree of analytical precision checked against the reference standard material (CH-6) by a multiple analysis was within a 0.1% range.

6.2.5 *Statistical Analysis*

At least five measurements were carried out on the ten sub-samples collected within a 1-m² range for each of the eight sampling areas, and their average values were used in all the statistical analyses. The analysis of variance (ANOVA) and canonical discriminant analysis were performed using SPSS 18.0, and other analyses such as partial least square (PLS) data analysis were performed using SIMCA. The level of reliability was kept at 95 % for all the analyses.

6.3 Results and Discussion

The average values resulting from the three experiments performed five times each on a total of 80 sub-samples (S and D of five spots [a, b, c, d, and e] of each of the eight areas) are listed in Tables 6.2 and 6.3.

6.3.1 *Color Determination*

A spectrophotometer furnishes the required data by quantifying the color tones with an accuracy better than that of human eye. The spectrophotometer used in this study can measure the wavelengths between 400 and 700 nm, measures the color attributes as Munsell's hue, value, and chroma in L*, a*, and b* (CIELAB index), respectively, and provide spectra along with reflectance data. The CIELAB color space, which was specified by the Commission Internationale de l'éclairage (CIE), has been internationally used as the standard color scale. It shows the color difference in delta E (ΔE) unit. In the CIELAB color space, L* represents luminance (brightness), and hue and intensity are expressed as a* and b* values. With a* and b*, the direction of a color is indicated: +a* indicates the direction toward red, -a* toward green, +b* toward yellow, and -b* toward blue (Fig. 6.3). The color intensity increases as the given value increases. While the human eye can usually detect color difference from 3 (ΔE) onwards, the spectrophotometer was calibrated to detect the color difference smaller than or equal to 1 (ΔE). The calibration was performed again for every analysis.

Table 6.2 The average data from 8 areas in Gangwon-do (S: on the surface, D: from a depth of 30 cm) using XRF

Data label	XRF						Fe ₂ O ₃ (%)						K ₂ O(%)						CaO(%)						TiO ₂ (%)											
	SiO ₂ (%)		Al ₂ O ₃ (%)		Fe ₂ O ₃ (%)		K ₂ O(%)		CaO(%)		TiO ₂ (%)		SiO ₂ (%)		Al ₂ O ₃ (%)		Fe ₂ O ₃ (%)		K ₂ O(%)		CaO(%)		TiO ₂ (%)		SiO ₂ (%)		Al ₂ O ₃ (%)		Fe ₂ O ₃ (%)		K ₂ O(%)		CaO(%)		TiO ₂ (%)	
	Ave	Std	RSD	Ave	Std	RSD	Ave	Std	RSD	Ave	Std	RSD	Ave	Std	RSD	Ave	Std	RSD	Ave	Std	RSD	Ave	Std	RSD	Ave	Std	RSD	Ave	Std	RSD	Ave	Std	RSD	Ave	Std	RSD
1-1-S	54.78	1.42	2.60	16.74	2.66	15.90	11.88	0.51	4.33	4.90	0.17	3.56	5.00	0.14	2.89	1.40	0.05	3.72																		
1-2-S	57.45	1.75	3.04	14.55	2.89	19.88	12.02	0.64	5.32	5.45	0.18	3.28	3.83	0.14	3.73	1.38	0.05	3.83																		
1-3-S	53.82	0.88	1.63	15.09	1.67	11.10	12.08	0.41	3.40	5.08	0.10	1.91	5.08	0.14	2.67	1.50	0.08	5.01																		
1-4-S	54.04	1.24	2.29	15.22	2.08	13.70	12.66	0.58	4.57	5.18	0.15	2.90	4.59	0.12	2.71	1.42	0.06	3.94																		
1-5-S	54.26	1.37	2.52	16.23	2.32	14.29	13.10	0.61	4.66	5.12	0.12	2.42	4.98	0.14	2.79	1.47	0.06	3.91																		
1-1-D	55.99	2.13	3.81	16.18	3.87	23.91	11.57	0.71	6.12	5.17	0.25	4.76	5.10	0.22	4.21	1.34	0.06	4.60																		
1-2-D	55.55	1.33	2.40	18.32	2.03	11.08	11.15	0.39	3.47	5.24	0.19	3.58	3.90	0.11	2.79	1.27	0.04	3.31																		
1-3-D	56.28	2.28	4.06	14.76	4.90	33.20	11.92	1.17	9.80	5.13	0.35	6.73	5.30	0.39	7.37	1.44	0.14	9.58																		
1-4-D	57.06	1.37	2.39	13.86	3.18	22.93	12.63	0.80	6.35	5.37	0.23	4.24	4.52	0.24	5.35	1.46	0.07	4.53																		
1-5-D	55.28	1.41	2.55	16.19	2.26	13.94	11.76	0.41	3.50	5.11	0.17	3.25	5.02	0.14	2.79	1.50	0.07	4.81																		
1Area	55.45	1.25	2.26	15.71	1.29	8.18	12.08	0.57	4.74	5.18	0.15	2.98	4.73	0.51	10.85	1.42	0.07	5.13																		
2-1-S	55.16	1.18	2.14	15.82	2.30	14.51	10.15	0.40	3.89	4.79	0.16	3.33	4.14	0.17	4.02	1.35	0.05	3.96																		
2-2-S	58.19	2.23	3.83	12.18	4.28	35.09	11.50	0.95	8.28	5.40	0.31	5.80	4.47	0.32	7.22	1.51	0.11	7.37																		
2-3-S	55.98	2.11	3.76	13.15	4.48	34.06	11.05	0.83	7.51	4.86	0.27	5.56	4.37	0.28	6.40	1.37	0.08	5.62																		
2-4-S	55.49	1.35	2.44	14.26	2.53	17.77	11.14	0.48	4.27	4.85	0.18	3.68	4.50	0.16	3.54	1.44	0.03	2.12																		
2-5-S	58.12	0.88	1.52	16.81	2.00	11.92	9.32	0.44	4.72	5.39	0.24	4.51	4.17	0.18	4.29	1.30	0.06	4.28																		
2-1-D	54.52	1.57	2.89	15.69	3.38	21.55	12.87	0.84	6.56	4.35	0.19	4.31	5.46	0.28	5.05	1.63	0.10	6.29																		
2-2-D	57.47	0.74	1.30	13.51	1.35	9.99	11.83	0.29	2.46	4.72	0.14	2.93	5.79	0.17	3.02	1.47	0.03	2.05																		
2-3-D	57.49	1.88	3.27	16.00	4.39	27.45	10.22	0.98	9.62	5.09	0.41	8.12	4.39	0.35	7.89	1.28	0.12	9.64																		
2-4-D	58.00	0.76	1.32	13.60	2.70	19.83	10.42	0.87	8.37	5.23	0.25	4.82	4.70	0.28	5.95	1.41	0.07	5.09																		
2-5-D	62.14	1.78	2.86	11.99	3.22	26.83	8.65	0.45	5.24	6.26	0.30	4.81	4.03	0.25	6.30	1.16	0.06	5.25																		
2Area	57.26	2.18	3.81	14.30	1.69	11.81	10.71	1.23	11.49	5.09	0.52	10.27	4.60	0.58	12.55	1.39	0.13	9.35																		

(continued)

Table 6.2 (continued)

Data label	XRF																	
	SiO ₂ (%)			Al ₂ O ₃ (%)			Fe ₂ O ₃ (%)			K ₂ O(%)			CaO(%)			TiO ₂ (%)		
	Ave	Std	RSD	Ave	Std	RSD	Ave	Std	RSD	Ave	Std	RSD	Ave	Std	RSD	Ave	Std	RSD
3-1-S	60.19	2.36	3.91	14.05	4.36	31.07	7.86	0.53	6.74	5.40	0.30	5.54	2.05	0.08	4.09	1.22	0.10	8.45
3-2-S	63.16	2.17	3.43	13.05	3.62	27.75	6.26	0.42	6.69	6.57	0.35	5.40	2.59	0.18	7.04	0.94	0.05	4.85
3-3-S	61.33	1.72	2.80	13.84	3.15	22.76	6.92	0.39	5.67	6.68	0.34	5.11	2.78	0.17	6.10	1.04	0.05	4.99
3-4-S	59.39	1.77	2.97	12.47	3.13	25.11	8.97	0.47	5.24	6.05	0.19	3.21	2.87	0.12	4.17	1.15	0.05	4.29
3-5-S	64.55	1.69	2.61	13.07	2.88	22.01	6.60	0.33	5.03	7.51	0.38	5.07	2.44	0.13	5.17	1.07	0.07	6.98
3-1-D	64.62	1.07	1.66	11.25	2.41	21.42	6.81	0.41	5.97	7.14	0.24	3.40	3.14	0.19	5.92	1.03	0.04	4.36
3-2-D	64.84	1.01	1.56	11.36	2.33	20.55	5.14	0.26	5.10	6.56	0.21	3.18	2.50	0.11	4.60	0.76	0.04	5.59
3-3-D	64.81	2.81	4.34	11.52	4.88	42.41	6.96	0.64	9.20	6.86	0.50	7.26	3.05	0.25	8.17	1.06	0.07	6.77
3-4-D	61.88	1.88	3.04	15.02	2.77	18.44	6.33	0.30	4.77	6.45	0.33	5.10	2.97	0.09	3.04	0.98	0.06	5.72
3-5-D	60.82	0.80	1.32	15.93	1.23	7.74	6.80	0.17	2.49	6.36	0.14	2.20	2.94	0.08	2.78	1.03	0.04	3.50
3Area	62.56	2.09	3.35	13.16	1.58	12.01	6.86	1.01	14.66	6.56	0.58	8.79	2.73	0.34	12.29	1.03	0.12	11.89
4-1-S	53.31	1.51	2.84	15.91	3.14	19.74	11.79	0.64	5.45	4.89	0.20	4.01	4.41	0.21	4.73	1.43	0.08	5.25
4-2-S	54.49	2.35	4.31	14.52	5.19	35.74	13.06	1.23	9.44	4.88	0.40	8.11	4.09	0.32	7.76	1.35	0.09	6.66
4-3-S	64.14	1.64	2.56	14.34	2.52	17.58	4.24	0.22	5.20	7.96	0.30	3.76	0.96	0.07	7.08	0.73	0.03	4.45
4-4-S	53.15	0.95	1.79	17.70	1.78	10.06	12.81	0.38	2.94	4.78	0.14	2.95	3.97	0.09	2.28	1.39	0.01	1.07
4-5-S	54.14	0.97	1.79	16.98	2.16	12.70	12.53	0.66	5.26	5.16	0.22	4.32	3.47	0.10	2.86	1.45	0.06	4.27
4-1-D	59.93	2.43	4.06	13.72	4.70	34.25	9.90	0.95	9.58	6.12	0.41	6.75	3.56	0.28	7.97	1.31	0.12	9.47
4-2-D	61.44	2.00	3.25	14.52	3.59	24.74	7.32	0.53	7.27	6.94	0.38	5.42	2.35	0.12	5.13	1.02	0.07	6.37
4-3-D	65.54	1.53	2.34	13.61	2.36	17.31	3.61	0.16	4.43	7.95	0.30	3.74	0.85	0.04	4.71	0.67	0.05	6.81
4-4-D	61.81	2.40	3.88	11.76	4.55	38.68	8.84	0.71	8.08	6.62	0.41	6.16	2.64	0.22	8.22	1.13	0.10	8.61
4-5-D	56.88	1.77	3.11	15.52	3.54	22.83	12.02	0.90	7.48	5.15	0.26	4.97	3.54	0.20	5.79	1.51	0.09	6.00
4Area	58.48	4.67	7.99	14.86	1.74	11.68	9.61	3.53	36.70	6.05	1.26	20.84	2.98	1.26	42.27	1.20	0.30	25.22
5-1-S	64.23	1.38	2.14	15.17	2.16	14.22	4.67	0.23	4.98	8.28	0.23	2.84	0.91	0.05	5.71	0.71	0.04	5.63

5-2-S	66.62	2.38	3.58	10.44	3.83	36.63	5.24	0.31	5.85	8.69	0.35	4.04	0.88	0.03	3.41	0.78	0.08	10.65
5-3-S	61.67	1.12	1.82	16.33	2.02	12.38	4.63	0.27	5.75	7.39	0.38	5.11	1.08	0.16	14.58	0.72	0.04	5.21
5-4-S	65.21	1.77	2.72	13.07	3.22	24.60	5.09	0.36	7.16	8.58	0.50	5.77	0.80	0.06	7.82	0.75	0.05	6.27
5-5-S	62.79	2.53	4.02	16.34	4.12	25.24	5.05	0.40	7.87	7.92	0.53	6.70	1.06	0.06	5.43	0.81	0.05	6.62
5-1-D	64.78	1.98	3.06	14.10	3.30	23.44	4.59	0.26	5.71	7.94	0.38	4.84	0.79	0.03	4.40	0.69	0.04	6.43
5-2-D	63.74	2.10	3.29	17.29	3.15	18.21	4.76	0.33	6.85	8.03	0.39	4.84	0.81	0.03	3.54	0.68	0.05	6.90
5-3-D	64.20	2.30	3.59	12.93	4.04	31.25	4.69	0.38	8.17	8.00	0.40	5.05	0.83	0.07	8.34	0.73	0.07	9.27
5-4-D	65.87	3.06	4.64	13.04	4.70	36.07	4.85	0.46	9.46	8.50	0.57	6.67	0.86	0.06	7.28	0.73	0.07	9.06
5-5-D	64.97	2.65	4.07	11.84	4.81	40.59	4.89	0.37	7.52	8.13	0.55	6.75	0.85	0.11	13.37	0.75	0.08	10.19
5Area	64.41	1.44	2.24	14.05	2.19	15.60	4.85	0.22	4.51	8.15	0.38	4.70	0.89	0.10	11.71	0.74	0.04	5.27
6-1-S	56.49	1.36	2.40	16.28	2.98	18.33	7.84	0.35	4.50	6.56	0.26	4.02	1.39	0.06	4.23	1.23	0.06	4.84
6-2-S	56.05	3.05	5.43	14.92	5.93	39.76	9.62	0.99	10.30	6.01	0.43	7.18	1.62	0.16	9.62	1.37	0.12	8.74
6-3-S	57.83	2.61	4.51	13.76	4.94	35.91	8.70	0.67	7.67	6.60	0.38	5.84	1.27	0.08	6.01	1.38	0.11	8.06
6-4-S	55.51	2.35	4.24	17.53	4.14	23.64	8.17	0.48	5.93	6.39	0.21	3.29	1.39	0.09	6.50	1.22	0.08	6.87
6-5-S	57.81	1.50	2.59	16.41	3.09	18.81	7.83	0.36	4.61	7.20	0.36	4.97	0.89	0.07	8.35	1.19	0.08	6.75
6-1-D	61.23	1.93	3.16	13.21	3.22	24.36	7.44	0.36	4.78	7.86	0.36	4.60	0.76	0.05	6.05	1.17	0.05	4.37
6-2-D	58.15	1.94	3.33	17.52	3.44	19.65	8.64	0.57	6.55	7.79	0.40	5.17	0.73	0.06	7.70	1.34	0.08	6.22
6-3-D	60.36	1.11	1.84	14.24	1.73	12.15	7.67	0.27	3.54	7.79	0.24	3.13	0.70	0.05	7.59	1.20	0.03	2.13
6-4-D	60.41	1.89	3.13	13.44	3.43	25.51	8.27	0.52	6.26	7.91	0.33	4.23	0.86	0.04	4.10	1.32	0.10	7.36
6-5-D	61.41	1.87	3.04	13.58	3.56	26.21	9.08	0.65	7.17	8.33	0.45	5.37	0.75	0.04	5.23	1.40	0.09	6.71
6Area	58.53	2.19	3.74	15.09	1.70	11.28	8.33	0.68	8.20	7.24	0.80	11.04	1.04	0.34	33.20	1.28	0.09	6.83
7-1-S	63.14	2.52	4.00	13.96	3.68	26.36	6.07	0.37	6.05	5.71	0.27	4.75	3.38	0.20	5.81	0.88	0.06	6.65
7-2-S	62.46	1.60	2.56	14.85	2.68	18.02	6.40	0.32	5.03	5.62	0.21	3.74	3.29	0.14	4.26	0.90	0.04	4.67

(continued)

Table 6.2 (continued)

Data label	XRF																	
	SiO ₂ (%)			Al ₂ O ₃ (%)			Fe ₂ O ₃ (%)			K ₂ O(%)			CaO(%)			TiO ₂ (%)		
	Ave	Std	RSD	Ave	Std	RSD	Ave	Std	RSD	Ave	Std	RSD	Ave	Std	RSD	Ave	Std	RSD
7-3-S	67.51	1.84	2.73	9.37	3.00	32.04	5.57	0.30	5.40	5.97	0.34	5.73	3.38	0.16	4.71	0.95	0.06	6.83
7-4-S	62.59	2.19	3.50	11.01	4.42	40.12	7.94	0.66	8.37	5.76	0.37	6.41	3.71	0.22	5.81	1.07	0.08	7.62
7-5-S	66.04	1.34	2.02	10.49	3.78	36.05	6.41	0.65	10.06	6.37	0.41	6.37	3.46	0.26	7.65	0.94	0.09	9.67
7-1-D	65.98	1.09	1.64	12.23	1.49	12.17	5.14	0.15	2.86	6.07	0.12	1.97	3.22	0.09	2.92	0.92	0.02	2.66
7-2-D	66.14	1.84	2.78	12.68	3.11	24.52	4.78	0.27	5.65	5.48	0.27	4.97	3.14	0.22	6.96	0.89	0.07	7.45
7-3-D	67.74	2.62	3.86	6.94	4.77	68.63	7.03	0.63	8.89	6.78	0.48	7.14	3.18	0.19	6.10	0.91	0.04	4.48
7-4-D	66.26	2.55	3.86	9.94	4.12	41.51	5.99	0.44	7.28	6.40	0.34	5.25	3.22	0.23	7.08	0.89	0.06	6.45
7-5-D	66.33	0.92	1.39	10.34	2.17	21.02	5.73	0.18	3.07	6.56	0.18	2.79	2.96	0.14	4.88	0.81	0.02	2.31
7Area	65.42	1.96	2.99	11.18	2.32	20.77	6.11	0.92	14.99	6.07	0.44	7.24	3.29	0.20	6.20	0.92	0.07	7.43
8-1-S	55.39	1.25	2.25	16.51	2.36	14.32	11.03	0.41	3.76	5.17	0.17	3.27	3.78	0.11	3.01	1.30	0.03	2.60
8-2-S	56.19	1.29	2.30	13.14	2.88	21.94	11.65	0.63	5.42	5.46	0.24	4.41	4.10	0.21	5.05	1.35	0.08	5.54
8-3-S	55.61	0.51	0.92	12.86	1.44	11.16	11.64	0.33	2.84	5.45	0.15	2.81	4.14	0.17	4.23	1.35	0.06	4.15
8-4-S	55.58	1.63	2.93	14.87	3.00	20.19	11.21	0.52	4.65	5.18	0.20	3.85	4.21	0.17	4.05	1.31	0.05	3.66
8-5-S	56.47	1.89	3.35	14.46	3.50	24.23	10.99	0.59	5.38	5.40	0.25	4.59	4.35	0.19	4.40	1.33	0.06	4.78
8-1-D	60.83	2.11	3.46	13.09	3.50	26.73	9.16	0.53	5.74	5.84	0.32	5.54	3.54	0.13	3.53	1.15	0.06	4.83
8-2-D	62.52	1.90	3.04	12.02	3.25	27.02	8.42	0.50	5.95	6.33	0.31	4.95	3.46	0.15	4.28	1.10	0.06	5.28
8-3-D	61.87	1.20	1.93	12.01	2.63	21.92	8.62	0.51	5.94	6.16	0.30	4.88	3.81	0.20	5.19	1.17	0.06	4.79
8-4-D	60.64	1.91	3.14	13.00	3.05	23.47	9.08	0.57	6.28	6.07	0.21	3.48	3.82	0.18	4.60	1.21	0.07	5.66
8-5-D	62.17	2.44	3.92	12.44	4.61	37.02	8.56	0.75	8.73	6.16	0.42	6.89	3.70	0.26	7.00	1.20	0.11	9.35
8Area	58.73	3.10	5.28	13.44	1.43	10.61	10.04	1.37	13.66	5.72	0.44	7.65	3.89	0.29	7.57	1.25	0.09	7.37

Table 6.3 The average data from 8 areas in Gangwon-do(S: on the surface, D: from a depth of 30 cm) with a spectrophotometer and EA-IRMS

Data label	SpectraMagic NX												EA-IRMS					
	L*(D65)				a*(D65)				b*(D65)				$\delta^{13}C(\text{‰})$			C amount(%)		
	Ave	Std	RSD	RSD	Ave	Std	RSD	RSD	Ave	Std	RSD	Ave	Std	RSD	Ave	Std	RSD	
1-1-S	48.64	0.00	0.00	0.00	6.63	0.00	0.00	0.00	19.87	0.01	0.03	-25.85	0.21	-0.81	0.38	0.01	2.84	
1-2-S	50.02	0.00	0.00	0.00	6.90	0.01	0.08	0.05	20.09	0.01	0.05	-26.23	0.20	-0.76	0.31	0.01	2.56	
1-3-S	48.71	0.01	0.01	0.00	6.23	0.00	0.00	0.00	19.52	0.00	0.00	-26.56	0.05	-0.18	0.65	0.01	1.31	
1-4-S	48.91	0.01	0.01	0.01	6.55	0.00	0.00	0.00	19.92	0.01	0.05	-25.58	0.05	-0.18	0.69	0.02	3.29	
1-5-S	48.54	0.40	0.81	0.04	6.00	0.03	0.57	0.62	19.24	0.12	0.62	-25.89	0.20	-0.76	0.63	0.04	6.03	
1-1-D	51.37	0.02	0.04	0.04	6.85	0.01	0.08	0.14	20.31	0.03	0.14	-25.06	0.42	-1.68	0.19	0.01	3.92	
1-2-D	50.03	0.11	0.23	0.75	6.61	0.06	0.92	0.65	19.18	0.12	0.65	-26.25	0.23	-0.89	0.25	0.01	3.30	
1-3-D	49.91	0.38	0.75	0.36	6.20	0.02	0.36	0.63	19.11	0.12	0.63	-26.59	0.19	-0.73	0.44	0.04	8.88	
1-4-D	46.03	0.12	0.26	0.15	6.48	0.01	0.15	0.36	18.75	0.07	0.36	-25.57	0.30	-1.18	0.24	0.01	2.59	
1-5-D	47.14	0.25	0.54	0.62	6.46	0.04	0.62	0.08	18.95	0.02	0.08	-25.37	0.25	-0.99	0.14	0.01	9.93	
1Area	48.93	1.54	3.14	4.36	6.49	0.28	4.36	2.71	19.49	0.53	2.71	-25.89	0.51	1.98	0.39	0.20	51.44	
2-1-S	45.13	0.14	0.31	0.31	4.83	0.02	0.31	0.33	16.27	0.05	0.33	-23.82	0.37	-1.57	3.21	0.03	0.92	
2-2-S	50.51	0.13	0.26	0.39	5.93	0.02	0.39	0.33	19.59	0.07	0.33	-21.33	0.12	-0.56	1.12	0.01	0.66	
2-3-S	44.31	0.08	0.18	0.21	4.72	0.01	0.21	0.00	15.94	0.00	0.00	-23.54	0.14	-0.60	3.63	0.09	2.43	
2-4-S	47.39	0.11	0.23	0.50	4.99	0.03	0.50	0.15	17.33	0.03	0.15	-24.07	0.04	-0.16	2.86	0.05	1.88	
2-5-S	50.30	0.21	0.41	0.38	5.53	0.02	0.38	0.26	19.02	0.05	0.26	-22.18	0.53	-2.37	1.87	0.02	1.32	
2-1-D	49.88	0.23	0.47	0.18	6.42	0.01	0.18	0.29	20.85	0.06	0.29	-23.04	0.26	-1.13	0.74	0.04	5.18	
2-2-D	50.31	0.21	0.41	0.80	5.74	0.05	0.80	0.76	19.50	0.15	0.76	-21.42	0.21	-1.00	0.48	0.01	3.10	
2-3-D	50.22	0.04	0.07	0.10	5.74	0.01	0.10	0.06	19.26	0.01	0.06	-22.89	0.09	-0.39	1.28	0.01	0.81	
2-4-D	50.50	0.09	0.17	0.65	5.39	0.04	0.65	0.32	19.01	0.06	0.32	-23.97	0.02	-0.09	1.40	0.02	1.54	
2-5-D	54.01	0.05	0.10	0.61	5.75	0.04	0.61	0.09	20.01	0.02	0.09	-22.53	0.11	-0.51	0.55	0.00	0.31	
2Area	49.25	2.87	5.83	9.63	5.50	0.53	9.63	8.69	18.68	1.62	8.69	-22.88	1.01	4.40	1.71	1.14	66.54	

(continued)

Table 6.3 (continued)

Data label	SpectraMagic NX												EA-IRMS							
	L*(D65)				a*(D65)				b*(D65)				$\delta^{13}\text{C}(\text{‰})$							
	Ave	Std	RSD		Ave	Std	RSD		Ave	Std	RSD		Ave	Std	RSD		Ave	Std	RSD	
3-1-S	47.89	0.17	0.34		4.74	0.03	0.63		16.01	0.08	0.50		-25.93	0.07	-0.27		3.27	0.01	0.25	
3-2-S	49.06	0.00	0.00		4.64	0.00	0.00		15.91	0.00	0.00		-25.74	0.10	-0.37		2.73	0.08	2.98	
3-3-S	49.62	0.01	0.01		4.41	0.01	0.13		15.44	0.01	0.06		-25.63	0.08	-0.33		2.11	0.06	2.81	
3-4-S	48.45	0.09	0.19		4.53	0.04	0.89		15.72	0.09	0.57		-25.28	0.43	-1.70		2.17	0.08	3.52	
3-5-S	50.12	0.15	0.29		4.45	0.01	0.13		15.45	0.03	0.19		-25.64	0.02	-0.09		2.15	0.04	2.07	
3-1-D	49.08	0.03	0.06		4.61	0.04	0.76		16.22	0.06	0.36		-25.28	0.19	-0.75		1.44	0.02	1.72	
3-2-D	49.76	0.01	0.01		4.78	0.01	0.12		16.76	0.01	0.03		-24.99	0.07	-0.27		1.10	0.02	2.00	
3-3-D	50.58	0.16	0.32		4.86	0.05	1.04		16.86	0.07	0.44		-25.14	0.07	-0.30		0.99	0.03	2.98	
3-4-D	49.49	0.21	0.43		4.60	0.01	0.13		16.35	0.07	0.44		-25.21	0.04	-0.15		1.51	0.03	1.66	
3-5-D	48.31	0.05	0.10		4.55	0.02	0.34		16.11	0.02	0.09		-25.16	0.06	-0.22		1.67	0.06	3.38	
3Area	49.23	0.84	1.71		4.62	0.14	3.11		16.08	0.49	3.02		-25.40	0.31	1.22		1.91	0.72	37.44	
4-1-S	48.70	0.55	1.13		6.65	0.04	0.61		19.67	0.23	1.19		-25.40	0.34	-1.35		3.20	0.13	4.10	
4-2-S	49.04	0.05	0.10		7.53	0.06	0.74		21.12	0.20	0.92		-24.35	0.08	-0.33		1.60	0.04	2.33	
4-3-S	47.11	0.43	0.90		4.62	0.13	2.71		15.05	0.42	2.80		-21.01	0.11	-0.53		3.82	0.25	6.65	
4-4-S	49.18	0.05	0.10		7.52	0.02	0.31		21.16	0.04	0.17		-24.96	0.51	-2.02		1.31	0.03	2.49	
4-5-S	47.51	0.15	0.32		7.63	0.07	0.86		20.87	0.10	0.46		-27.45	0.14	-0.52		1.80	0.08	4.57	
4-1-D	51.01	0.27	0.53		6.72	0.11	1.67		19.99	0.16	0.78		-20.63	0.06	-0.31		1.26	0.06	5.09	
4-2-D	49.88	0.03	0.06		5.80	0.01	0.20		18.36	0.04	0.19		-21.42	0.08	-0.37		1.83	0.04	2.34	
4-3-D	51.45	0.01	0.01		5.32	0.01	0.11		17.45	0.01	0.03		-20.39	0.05	-0.23		2.08	0.13	6.01	
4-4-D	51.80	0.08	0.16		6.46	0.03	0.41		20.16	0.06	0.29		-21.08	0.08	-0.40		1.34	0.06	4.83	
4-5-D	54.51	0.29	0.53		8.61	0.06	0.64		23.45	0.14	0.60		-26.54	0.12	-0.47		0.56	0.03	5.45	
4Area	50.02	2.23	4.45		6.68	1.20	17.98		19.73	2.32	11.74		-23.32	2.69	11.54		1.88	0.97	51.37	
5-1-S	46.45	0.01	0.01		4.67	0.01	0.21		14.73	0.01	0.04		-24.69	0.10	-0.41		2.71	0.05	1.85	

5-2-S	47.55	0.11	0.23	4.74	0.05	1.12	15.00	0.13	0.85	-25.15	0.06	-0.23	2.46	0.04	1.47
5-3-S	46.74	0.00	0.00	4.78	0.01	0.12	15.04	0.01	0.04	-25.52	0.04	-0.17	2.48	0.05	2.19
5-4-S	45.97	0.45	0.98	4.61	0.04	0.88	14.48	0.11	0.79	-24.24	0.07	-0.30	2.70	0.06	2.05
5-5-S	47.20	0.05	0.11	4.88	0.01	0.24	15.43	0.01	0.06	-25.23	0.07	-0.27	2.69	0.10	3.72
5-1-D	47.11	0.00	0.00	4.93	0.01	0.12	15.14	0.01	0.04	-25.38	0.06	-0.24	2.51	0.06	2.26
5-2-D	48.16	0.27	0.56	4.98	0.07	1.45	15.72	0.15	0.97	-25.32	0.03	-0.12	1.99	0.07	3.49
5-3-D	48.75	0.01	0.01	4.99	0.01	0.12	15.64	0.01	0.07	-25.42	0.13	-0.52	1.92	0.07	3.67
5-4-D	47.22	0.07	0.15	4.75	0.03	0.53	14.85	0.03	0.17	-25.28	0.06	-0.23	2.51	0.04	1.41
5-5-D	47.37	0.00	0.00	4.83	0.01	0.12	14.88	0.01	0.04	-25.46	0.06	-0.24	2.66	0.07	2.54
5Area	47.25	0.80	1.69	4.82	0.13	2.67	15.09	0.40	2.65	-25.17	0.40	1.59	2.46	0.28	11.55
6-1-S	48.05	0.01	0.01	5.41	0.01	0.11	17.16	0.01	0.03	-25.07	0.05	-0.21	2.21	0.04	1.90
6-2-S	49.18	0.07	0.13	5.24	0.02	0.29	17.34	0.02	0.09	-25.11	0.08	-0.31	2.18	0.09	4.35
6-3-S	46.93	0.38	0.80	5.30	0.05	0.93	17.08	0.14	0.83	-24.78	0.34	-1.39	2.66	0.06	2.32
6-4-S	47.78	0.22	0.45	5.14	0.02	0.34	17.08	0.04	0.24	-24.87	0.34	-1.36	1.77	0.05	2.98
6-5-S	48.22	0.01	0.01	5.85	0.00	0.00	17.66	0.01	0.03	-24.04	0.04	-0.16	1.72	0.01	0.44
6-1-D	50.42	0.00	0.00	6.88	0.01	0.08	19.67	0.01	0.03	-22.66	0.16	-0.69	0.92	0.04	4.22
6-2-D	49.50	0.13	0.26	6.80	0.03	0.44	19.62	0.06	0.28	-23.41	0.38	-1.62	1.15	0.02	1.44
6-3-D	51.17	0.00	0.00	7.10	0.01	0.08	20.60	0.01	0.03	-23.05	0.19	-0.81	0.96	0.02	1.99
6-4-D	49.63	0.06	0.11	6.22	0.02	0.33	18.98	0.04	0.19	-24.07	0.05	-0.21	1.33	0.04	3.37
6-5-D	49.54	0.06	0.11	7.01	0.03	0.46	19.68	0.04	0.19	-23.01	0.05	-0.20	0.93	0.06	6.27
6Area	49.04	1.29	2.63	6.10	0.80	13.15	18.49	1.36	7.34	-24.01	0.93	3.86	1.58	0.62	39.26
7-1-S	53.99	0.22	0.40	3.87	0.13	3.27	15.26	0.08	0.49	-24.91	0.16	-0.63	0.76	0.01	1.77
7-2-S	54.24	0.30	0.56	3.98	0.06	1.45	15.52	0.04	0.28	-25.12	0.31	-1.25	0.95	0.08	8.39

(continued)

Table 6.3 (continued)

Data label	SpectraMagic NX												EA-IRMS					
	L*(D65)				a*(D65)				b*(D65)				$\delta^{13}\text{C}(\text{‰})$			C amount(%)		
	Ave	Std	RSD		Ave	Std	RSD		Ave	Std	RSD		Ave	Std	RSD	Ave	Std	RSD
7-3-S	54.00	0.08	0.14		3.94	0.07	1.69		15.54	0.20	1.31		-24.92	0.11	-0.43	0.74	0.04	5.36
7-4-S	53.25	0.03	0.05		4.06	0.09	2.29		15.71	0.16	1.01		-25.24	0.12	-0.47	1.13	0.05	4.68
7-5-S	53.07	0.13	0.24		4.01	0.03	0.66		15.61	0.02	0.11		-25.04	0.07	-0.28	0.75	0.05	6.39
7-1-D	54.16	0.32	0.58		4.03	0.11	2.74		15.88	0.22	1.36		-25.76	0.19	-0.76	0.84	0.06	7.26
7-2-D	55.21	0.87	1.58		4.15	0.03	0.74		16.00	0.10	0.63		-25.81	0.24	-0.94	0.62	0.03	5.22
7-3-D	48.37	0.42	0.86		4.42	0.01	0.23		16.36	0.05	0.32		-25.78	0.08	-0.31	1.22	0.11	8.68
7-4-D	51.77	0.00	0.00		4.49	0.01	0.22		16.54	0.01	0.03		-25.71	0.07	-0.29	1.36	0.10	7.04
7-5-D	51.38	0.01	0.01		4.17	0.00	0.00		16.46	0.00	0.00		-25.96	0.14	-0.53	1.61	0.14	8.76
7Area	52.94	1.98	3.74		4.11	0.20	4.93		15.89	0.44	2.78		-25.43	0.41	1.63	1.00	0.32	32.15
8-1-S	50.14	0.10	0.20		4.60	0.03	0.55		16.98	0.05	0.28		-25.76	0.45	-1.75	1.04	0.02	2.13
8-2-S	50.84	0.14	0.28		4.37	0.03	0.61		16.34	0.05	0.28		-25.30	0.16	-0.65	1.17	0.07	5.92
8-3-S	51.12	0.12	0.24		4.38	0.02	0.35		16.04	0.08	0.51		-24.73	0.16	-0.64	0.68	0.02	3.44
8-4-S	51.21	0.28	0.54		4.57	0.04	0.88		16.46	0.05	0.28		-24.95	0.16	-0.66	0.76	0.02	2.49
8-5-S	52.44	0.27	0.51		4.56	0.05	1.05		16.47	0.06	0.35		-24.72	0.05	-0.21	0.70	0.02	3.14
8-1-D	49.18	0.00	0.00		4.92	0.01	0.12		17.00	0.00	0.00		-26.11	0.07	-0.28	1.67	0.03	1.84
8-2-D	49.51	0.00	0.00		4.73	0.01	0.12		16.98	0.01	0.03		-25.63	0.17	-0.66	1.18	0.06	5.04
8-3-D	48.69	0.00	0.00		4.53	0.01	0.13		16.65	0.01	0.03		-25.93	0.11	-0.41	1.25	0.01	0.89
8-4-D	49.60	0.21	0.41		4.93	0.03	0.59		17.04	0.09	0.51		-25.73	0.08	-0.31	1.09	0.03	2.65
8-5-D	49.85	0.19	0.37		4.50	0.03	0.71		16.38	0.14	0.83		-26.03	0.07	-0.25	1.35	0.01	1.08
8Area	50.26	1.13	2.25		4.61	0.20	4.24		16.63	0.35	2.09		-25.49	0.53	2.08	1.09	0.31	28.66

CIE L*a*b*

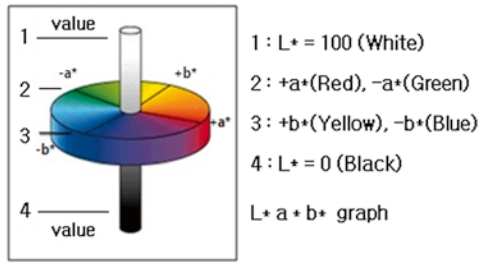


Fig. 6.3 CIELAB color space

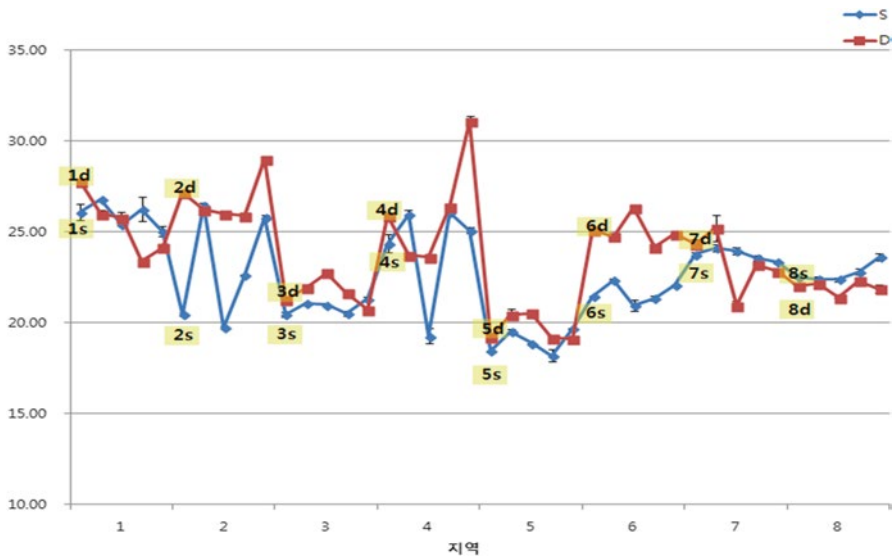


Fig. 6.4 Color differences between surface (S) and 30-cm depth (D)

While the color changes between the surface (S) and 30-cm depth (D) show similar patterns, as shown in Fig. 6.4, one area showed an S–D difference as large as 2.8 (ΔE). On the other hand, in some cases, similar color data could be obtained from different areas. For example, Area 1 and 2 are approximately 1 km apart from each other on either side of the river; however, 1-S, 1-D, and 2-D samples demonstrated strikingly similar color tones (Table 6.4). This implies that color tone should not be the sole factor for the identification of forensic soil samples.

As shown in Table 6.3, the areas which demonstrated the largest differences in color data between maximum and minimum values are Area 2 (L*) and Area 4 (a*, b*): L* (brightness) of Area 2 ranged from 44.31 to 54.01, and a* and b* of Area 4 ranged from 4.62 to 8.61 and from 15.05 to 23.45, respectively.

Table 6.4 Results of color measurements using spectrophotometer

Area	Label	S		D		Area	Label	S		D	
		Ave	Std.	Ave	Std.			Ave	Std.	Ave	Std.
1	1-1	26.09	0.44	27.75	0.01	5	5-1	18.43	0.01	19.19	0.01
	1-2	26.77	0.00	26.02	0.18		5-2	19.50	0.13	20.44	0.29
	1-3	25.39	0.00	25.79	0.32		5-3	18.87	0.01	20.52	0.01
	1-4	26.23	0.67	23.39	0.12		5-4	18.18	0.33	19.17	0.02
	1-5	25.02	0.28	24.13	0.12		5-5	19.67	0.03	19.10	0.01
2	2-1	20.47	0.08	27.15	0.18	6	6-1	21.44	0.01	25.12	0.01
	2-2	26.45	0.13	26.21	0.22		6-2	22.35	0.06	24.75	0.12
	2-3	19.75	0.04	25.98	0.03		6-3	20.95	0.31	26.32	0.00
	2-4	22.62	0.04	25.89	0.07		6-4	21.35	0.14	24.15	0.05
	2-5	25.80	0.10	29.00	0.05		6-5	22.06	0.01	24.89	0.07
3	3-1	20.46	0.15	21.28	0.05	7	7-1	23.76	0.11	24.33	0.24
	3-2	21.04	0.00	21.92	0.01		7-2	24.13	0.20	25.20	0.72
	3-3	20.97	0.01	22.74	0.04		7-3	23.96	0.19	20.93	0.28
	3-4	20.50	0.12	21.62	0.19		7-4	23.55	0.15	23.19	0.01
	3-5	21.31	0.12	20.72	0.04		7-5	23.35	0.07	22.81	0.00
4	4-1	24.36	0.48	25.87	0.07	8	8-1	22.50	0.10	22.02	0.01
	4-2	25.97	0.21	23.72	0.05		8-2	22.41	0.12	22.14	0.01
	4-3	19.26	0.42	23.60	0.01		8-3	22.38	0.11	21.37	0.00
	4-4	26.07	0.07	26.40	0.09		8-4	22.79	0.16	22.30	0.19
	4-5	25.08	0.17	31.08	0.29		8-5	23.61	0.20	21.85	0.23

Area 6 showed large deviations for a^* and b^* in both S and 30-cm D, whereas Area 1 showed the least deviation owing to a high degree of soil homogeneity.

The paired t -test on the results of color measurements confirmed that S and D samples showed significant differences in all L^* , a^* , and b^* ($p \leq 0.05$).

A canonical discriminant analysis was performed using the color attributes (L^* , a^* , and b^*) obtained from the above spectrophotometric analysis. Prior to the analysis, Box's M test was conducted to check the homogeneity of the multivariate normal covariance matrices of the three independent color variables (L^* , a^* , and b^*) for each group. Because the significance probability was estimated to be 0.000 indicating the lack of between-group homogeneity of covariance matrices, individual-group covariance matrices were utilized when applying the classification method.

The canonical discriminant analysis was performed using a stepwise method for selecting variables to be included in the analysis, where the significance of the variables entering in each step was tested using Wilks' lambda and exact F statistics. Therefore, all the variables were confirmed to have significance. The order of entrance was a^* (red direction) $\Rightarrow b^*$ (yellow direction) $\Rightarrow L^*$.

Out of the two canonical discriminant functions that were obtained in the discriminant analysis, the eigenvalue of Function 1 was 4.345, accounting for 54.6% of the total discriminating power. Thus, 100% discriminating ability was achieved by adding the discriminating ability of Functions 2 and 3 to that of Function 1.

These discriminant functions were subjected to significance tests and proved their significance, their significance probability being 0.000 each with respect to Wilks' lambda values and Chi-square statistic.

When referenced to the standardized canonical-discriminant-function coefficients, discriminant functions 1, 2, and 3 are most closely related to a^* , b^* , and L^* , respectively.

In the case of unstandardized coefficients, the standardized canonical discriminant functions were used to calculate the discriminant scores of individual samples, thereby acquiring the group centroids by entering the average value of each group.

The three discriminant functions utilized are as follows:

$$D1 = 11.152 - 0.175L^* + 4.037a^* - 1.378b^*$$

$$D2 = -4.555 - 0.440L^* - 3.837a^* + 2.683b^*$$

$$D3 = -26.317 + 0.596L^* + 1.691a^* - 0.703b^*$$

The centroids thus obtained demonstrated that Function 1 was effective in discriminating Area 7 and 4 from the other areas, and Function 2 was effective in discriminating Area 5 from others.

While the discrimination performed using the canonical discriminant functions confirmed a perfectly accurate classification of Area 2, 5, 6, and 8, Area 1, 3, 4, and 7 showed 2, 2, 5, and 1 classification errors out of 10, respectively, resulting in an overall classification accuracy of 87.5%.

Figure 6.5 is a scatter plot of discriminant scores calculated by using the canonical discriminant functions. The concentrated distribution of pink-colored plots in Area 8 demonstrates its relatively high classification accuracy. In particular, a clustering tendency is observed according to area-specific characteristics as follows: Area 3, 7, and 8 near the river; Area 1 and 2 near the industrial complex; Area 6 in the pasturage near factories; and Area 5 in the fishing zone. The broadest dispersion of discriminant scores is shown by Area 4, the roadsides near the residential areas, represented by violet color on the scatter plot.

Color factor b^* is related to yellow (Fig. 6.6). The color factor has a high degree of discriminating ability. Because soils of different colors are found even in an area as small as 1 m², samples should be taken from many different spots within the determined range, where due attention should be paid to different colors by a rough visual examination.

6.3.2 Elemental Analysis

The XRF analyses revealed the differences in soil elements from a sampling spot to another within the same area. The data are listed in Table 6.2.

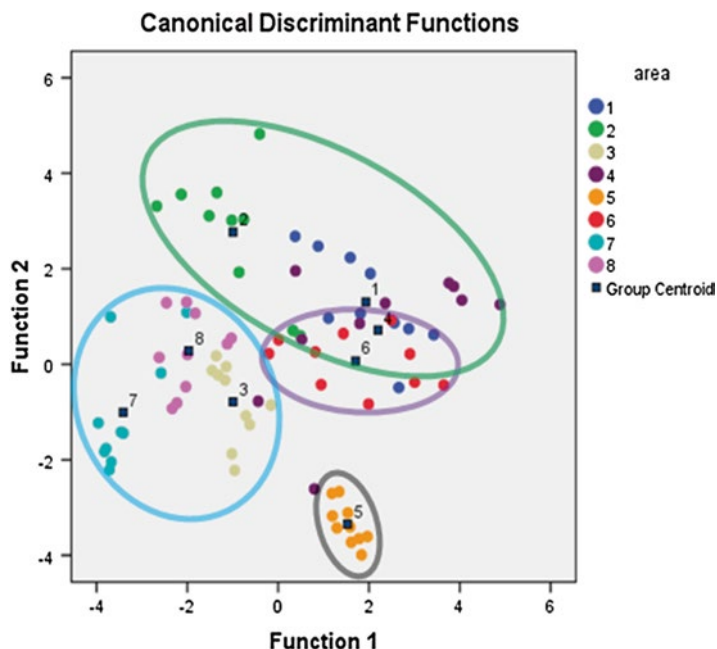


Fig. 6.5 Discriminant scores calculated with canonical discriminant functions

The smallest and largest differences in the distribution of elements for each sampling area were shown by SiO_2 in Area 4 with 53.15–65.54 %, Fe_2O_3 in Area 4 with 3.61–13.06 %, and Al_2O_3 in Area 7 with 6.94–14.85 %, respectively.

Significant S–D differences in element distribution were also confirmed among the surface and 30-cm depth samples within 1-m² range of the same area. The comparisons of the S–D data indicated that Area 8 contained 55.8 % and 61.6 % SiO_2 on average in its surface and depth soils, respectively, and 11.3 % and 8.7 % Fe_2O_3 in its surface and depth soils (Fig. 6.7).

The results of the paired *t*-test performed on the soil elements of both S and D samples confirmed that the Al_2O_3 content exhibited a significant depth-dependent difference.

A canonical discriminant analysis was then performed using the values of SiO_2 , Al_2O_3 , Fe_2O_3 , K_2O , CaO , and TiO_2 obtained from the elemental analyses.

Box's M test, which was conducted to test the homogeneity of the between-group covariance matrices of the six independent variables, namely, SiO_2 , Al_2O_3 , Fe_2O_3 , K_2O , CaO , and TiO_2 , gave a significance probability of 0.000. Since it signifies that there is no homogeneity of covariance matrices among the groups, the individual-group covariance matrices were utilized when applying the classification method.

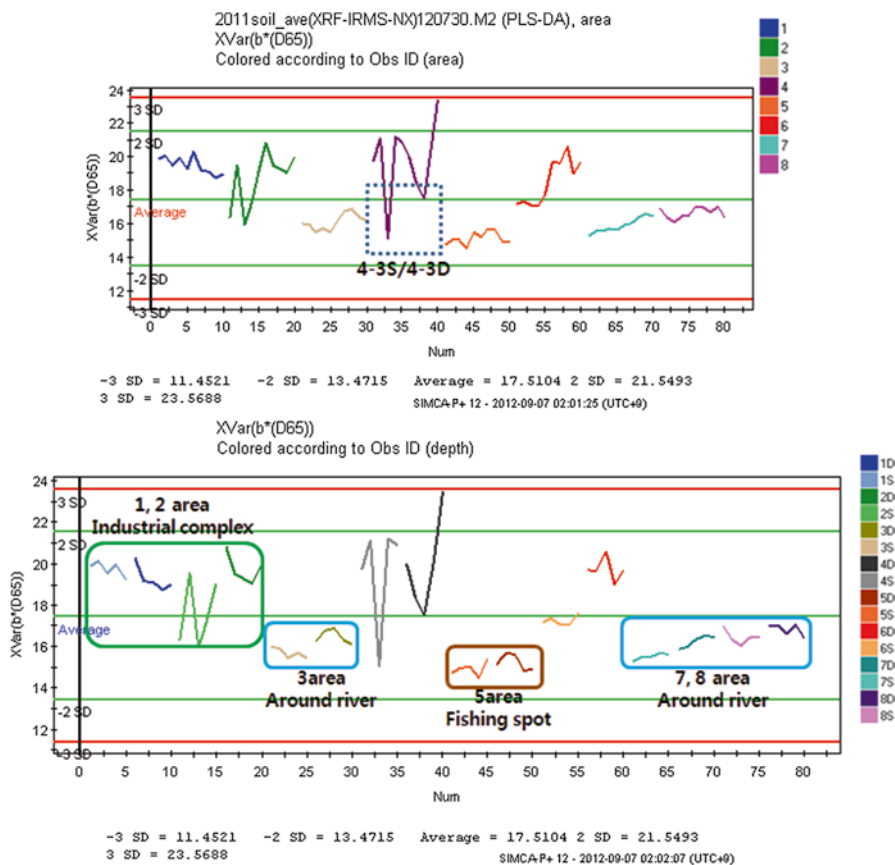


Fig. 6.6 Distribution diagram of color factor b^* by sampling area

The canonical discriminant analysis was performed using a stepwise selection method, where the significance of the variables entering in each step was tested using Wilks' lambda and exact F statistics. According to the results of significance tests, CaO was entered first, followed by TiO_2 and Fe_2O_3 . It is also shown that the variables entered had not been removed because of high values of F statistic.

Out of the two canonical discriminant functions that were obtained from the discriminant analysis, the eigenvalue of Function 1 is 9.915, thereby accounting for 71.3 % of the total discriminating power. Thus, 100 % discriminating power is possible by adding the discriminating power of Functions 2 and 3 to that of Function 1. The significance tests, which were performed on these discriminant functions, confirmed their significance probability as being 0.000 each with respect to Wilks' lambda values and Chi-square statistic.

The standardized canonical-discriminant-function coefficients show that the discriminant functions 1, 2, and 3 are most closely related to CaO, TiO_2 , and Fe_2O_3 , respectively.

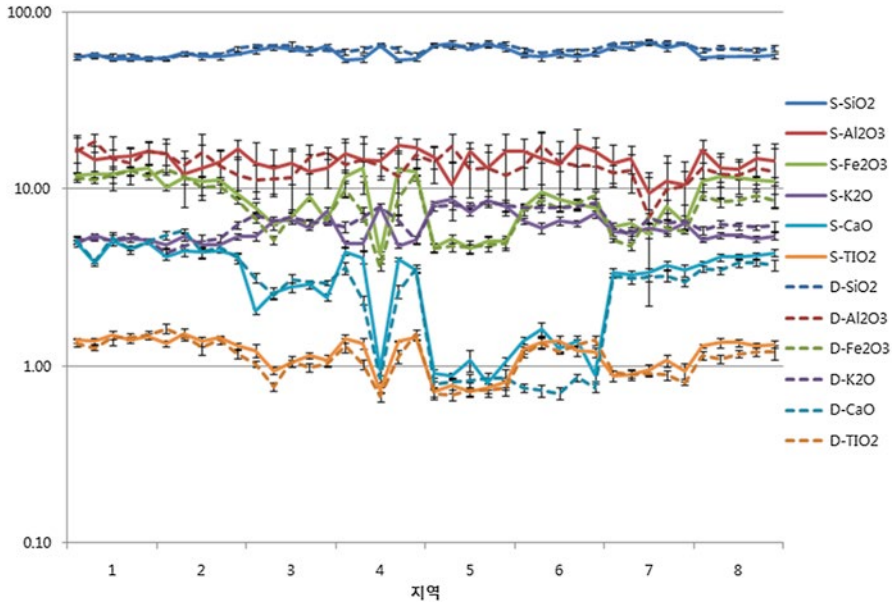


Fig. 6.7 Depth-dependent differences in soil element compositions (s: solid line, d: dash line)

The three discriminant functions utilized are as follows:

$$D1 = 0.355 - 0.158 Fe_2O_3 + 2.813 CaO - 6.502 TiO_2$$

$$D2 = -9.396 - 0.367 Fe_2O_3 - 0.141 CaO + 11.251 TiO_2$$

$$D3 = 3.165 + 1.718 Fe_2O_3 - 0.743 CaO - 13.579 TiO_2.$$

According to the centroid values, Function 1 was effective in discriminating Area 6 from other areas. Function 1 is easily influenced by CaO, and soils in Area 6, the pasture grounds near a factory, have relatively low CaO values compared to the other areas. The TiO₂-sensitive Function 2 is effective in discriminating Area 5 from the other areas because Area 5 is the fishing areas located near the dam that has soils with a low TiO₂ content.

The discrimination tests performed using the canonical discriminant functions confirmed a perfect classification of Area 5, 6, 7, and 8; however, revealed 2, 2, 1, 4 classification errors in Area 1, 2, 3, and 4, respectively, yielding an overall classification accuracy of 88.8%.

Figure 6.8 shows a scatter plot of the discriminant scores of the eight areas calculated by using the canonical discriminant functions. The distributions patterns

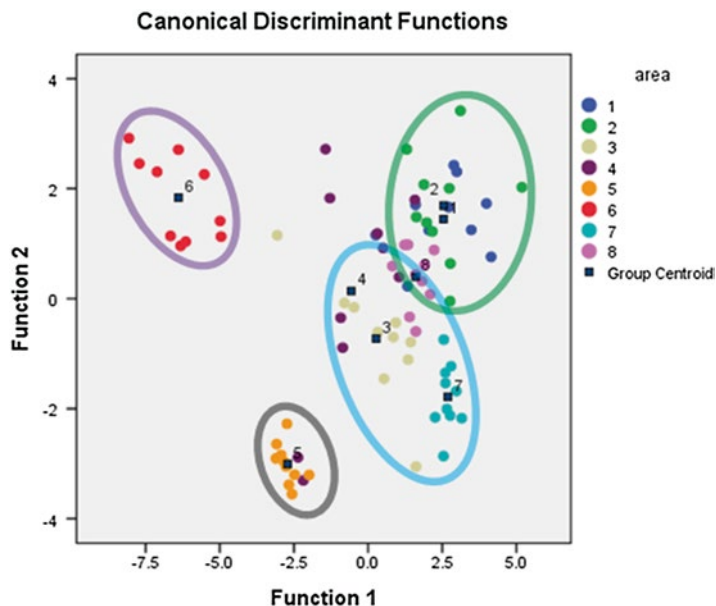


Fig. 6.8 A scatter plot illustrating the distribution of soil elements in the eight sampling plots

show a clear area-to-area discrimination. As shown in the results of color test, a clustering tendency is observed according to area-specific characteristics: Area 3, 7, and 8 near the river; Area 1 and 2 near the industrial complex, Area 6 near the pasturage of the factories, and Area 5 near the fishing zone of the dam.

The Fe_2O_3 content was found to be low in water areas. TiO_2 was found to be abundant in Area 1, 2, and 6. The SiO_2 content was found to be higher in Area 3, 5, 7, and 8-D than in other areas. It is noteworthy that the areas 1, 2, and 8-S showed similar distributions (Fig. 6.9). This indicates that the depth of soil influences the soil characteristics even within the same area.

In the SIMCA analysis according to depth (Fig. 6.10), the loading plot quadrants are divided between 8S (3rd quadrant) and 8D (4th quadrant). Either side of the y-axis is occupied by the manufacturing and industrial complex (1st and 4th quadrants) and the water areas (2nd and 3rd quadrants). Moreover, y-axis is a dividing line for the areas influenced by SiO_2 , Fe_2O_3 , and TiO_2 contents.

Water areas are typically formed with alluviums and considered to have high SiO_2 content. (Alluviums are unsolidified sediments shaped by the accumulation of soils consisting of gravel, sand, clay, etc. through recent river activities. Sand has mainly rock-forming mineral particles containing SiO_2 or Si; however, calcareous sands are also formed from limestones.)

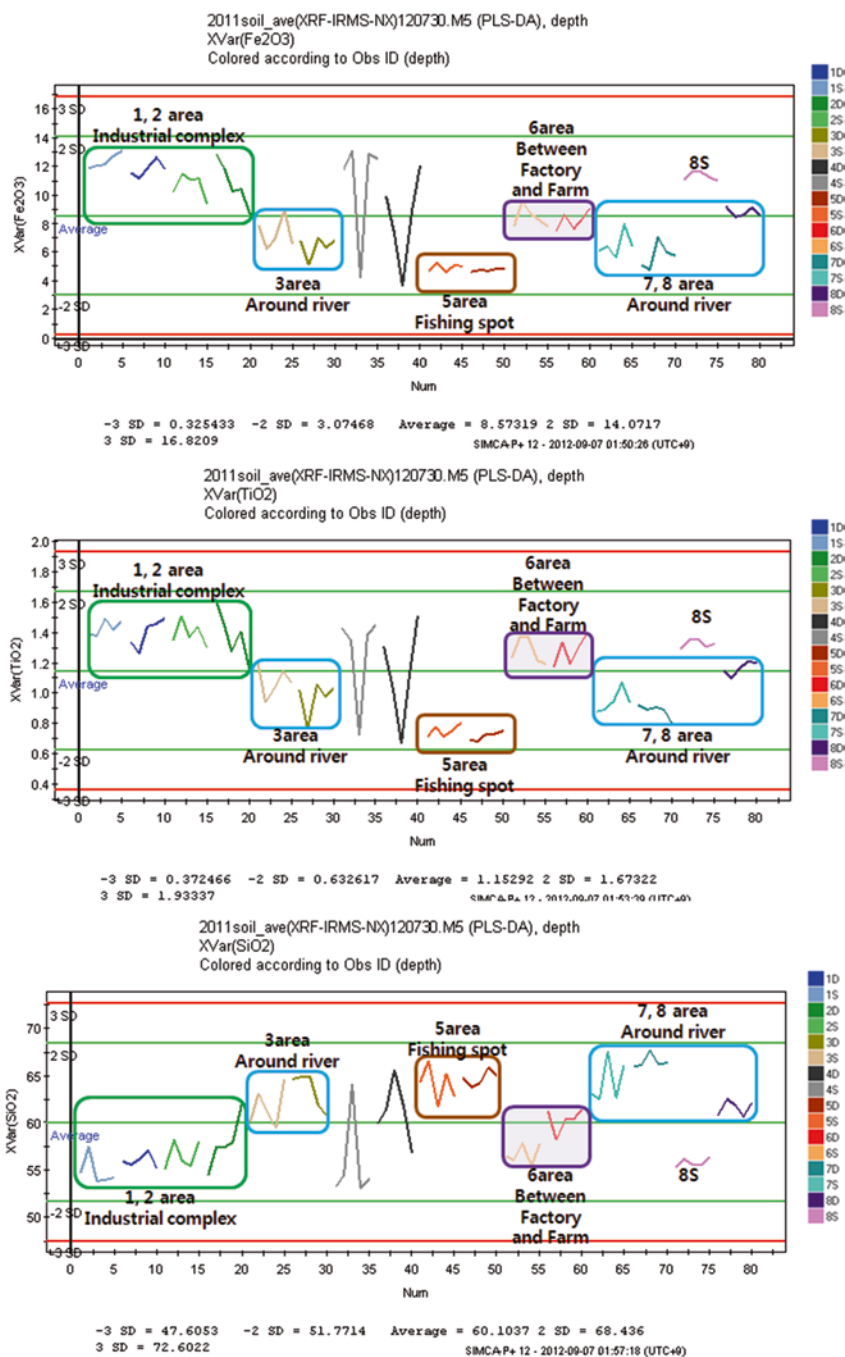


Fig. 6.9 Distribution diagrams of XRF measurement values by sampling area

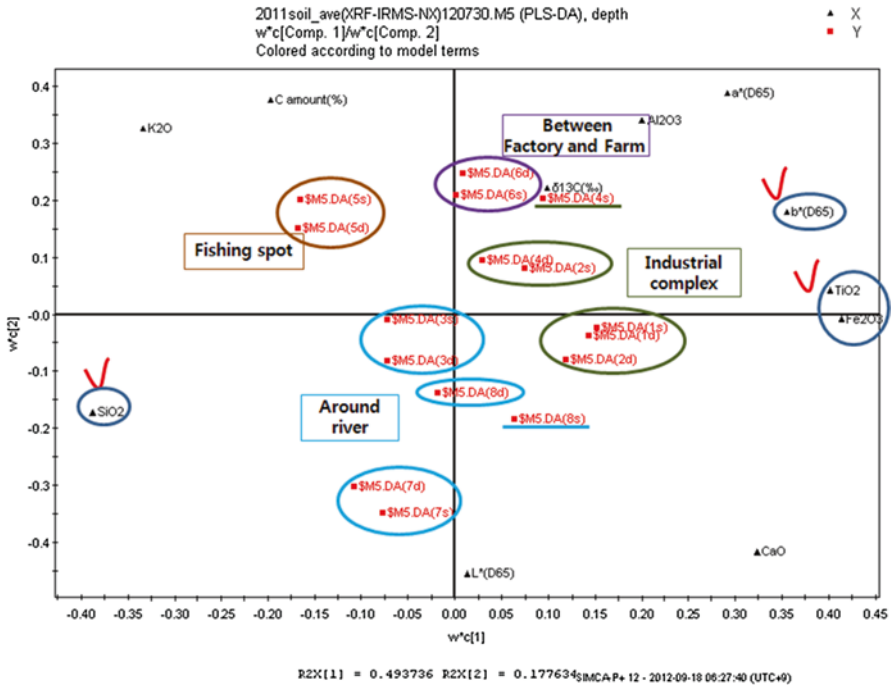


Fig. 6.10 Results of the SIMCA analysis

6.3.3 Carbon Isotope Ratio and Carbon Content

Figure 6.11 shows the carbon content and carbon-isotope ratio. A rough contrast between the river and industrial areas is observed. This contrast in carbon-isotope ratio distribution is also shown in the ANOVA. Group A is the water area consisting of Area 3, 5, 7, and 8. Consequently, the soils in the water area showed enrichment in isotope ratio compared to those in the industrial area.

The paired *t*-test on the results of carbon content and carbon-isotope ratio measurements of the S and D samples confirmed that the carbon content showed significant depth-dependent differences (0.000), whereas the carbon isotope ratio (0.64) was not influenced.

The results of depth analysis show that the carbon-isotope ratios were enriched in the D samples compared to the S samples in Area 1, 2, 3, 4, and 6, and the opposite was true for Area 5, 7, and 8.

The carbon content was higher in the S samples of Area 1–6, and in the D samples of Area 7 and 8. This contradictory result for Area 7 and 8 compared to all the other areas may be attributed to the influence of water flowing right next to the areas.

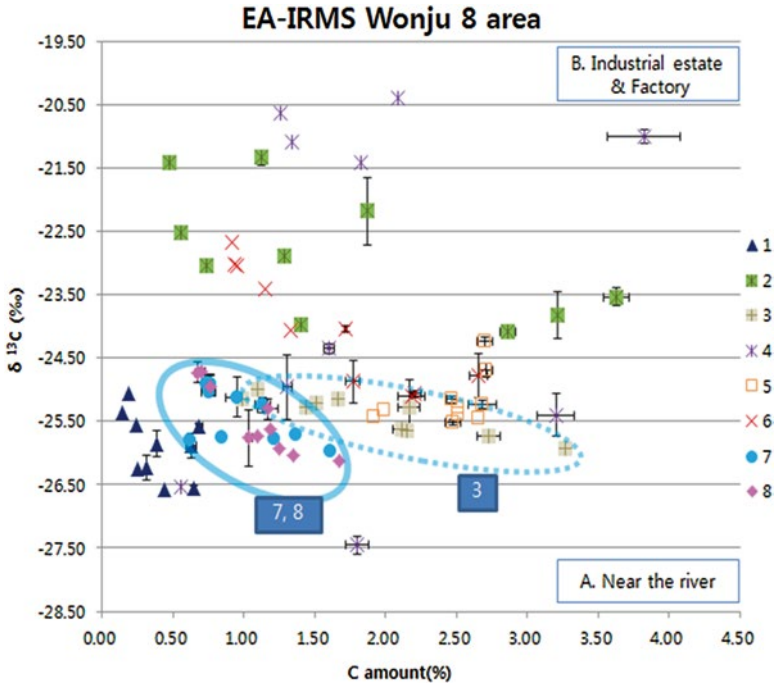


Fig. 6.11 Carbon amount (%) and carbon isotope ratio

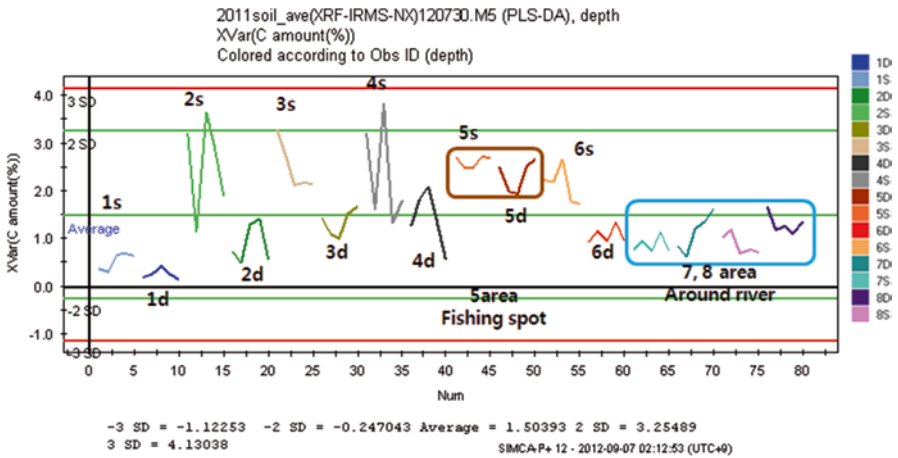


Fig. 6.12 Variable line plot of carbon amount (%) by area and depth

Figure 6.12 shows the carbon amount (%) in variable line plot that gives the measurement values of analysis factors grouped by areas (1–8) and depths (S and D) in different colors.

Because not only area-to-area, but also surface-to-depth differences were observed in all the measurements, therefore, when collecting comparative samples, due care should be taken to prevent the mixing of adjacent soils from the depths other than the expected depth.

6.3.4 Total Statistics

Principal Component Analysis (PCA)

PCA algorithm is a 2nd-order statistics that utilizes the statistical characteristics of mean values and sampling distributions. It searches for a series of orthonormal subsets indicating each direction of the maximum covariance for the input data. PCA is a standard tool for dimension reduction of correlated multivariate data while keeping the highest possible number of variables. This enables to create a new combination of variables, namely, a set of principal components (PC) converted from a set of variables. The PCs are linearly uncorrelated, and the first several ones are defined to carry out most of the changes that occurred in the original variables. PCA aims to extract and interpret a small number of PCs independent of one another by carrying out an adequate linear transformation of correlated variables in the cases where a direct interpretation of correlations among a number of images is difficult. The coordinates of PCs obtained from dimension reduction serve as input data for statistical analyses, thus playing an intermediate role in a series of analysis process (Park et al. 2011). Figure 6.13 shows the results of PCA-X statistics.

Each area is differentiated well according to its characteristics. In order to determine the area-specific determinant factors more accurately, a partial least squares-discriminant analysis (PLS-DA) was performed.

PLS-DA of Soils

The PLS-DA maximizes the covariance between the predicted data set (X block: unlimited number of soil factors) and the data to be predicted (Y block: class assignment). The fractions of the Y variables designed by the selected component and those predictable by the component determined by the cross validation were plotted, and the PLS-DA model thus constructed was validated. The predictions shown on the PLS-DA scatter plot are selected according to the significance rule specified by SIMCA-P software, where Q^2 of a significant component should be >0.05 for 100 observations or less and zero for more than 100 observations. Moreover, PLS-DA plots are displayed by the superposition of the two highest latent variables ($t[1]/t[2]$ or $p[1]/p[2]$ as x- and y-axes). The high coefficient values of R^2Y and Q^2Y indicate good discriminating power.

The soil discriminant factors can be obtained by observing the clustering of the input factors on a score plot using the PLS-DA multivariate analysis, thereby

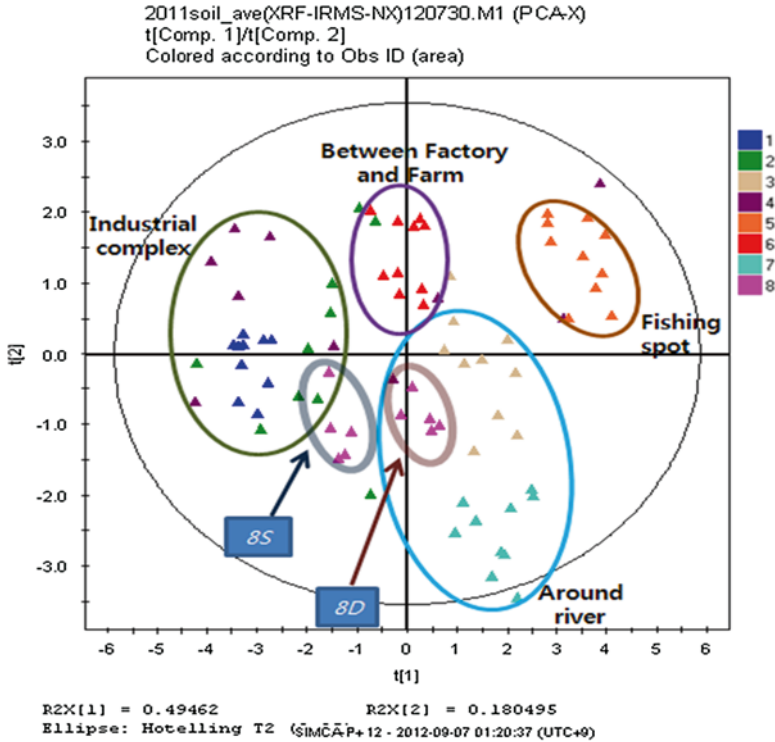


Fig. 6.13 Results of PCA-X statistics(S: on the surface, D: from a depth of 30 cm)

investigating the factors that are likely to be the indicators displayed on the loading plot, and finally having their significances confirmed using variable importance in the projection (VIP) (Kim 2007).

The degree of between-group discriminating accuracy can be assessed by comparing the spots within the 95 %-level confidence ellipses on the score plot. The results of the analyses of the soil samples of the eight areas in Wonju (Gangwondo, South Korea) were plotted on a PLS-DA score plot (Fig. 6.14), and the clustering patterns were observed. Therefore, they were classified into four groups according to the area-specific characteristics, whereby Area 8 was divided into two different groups because of the S–D differences.

After the results of the score plot were analyzed, the loading plot was then examined to identify the determinant factors by quadrant that displayed the distribution of each area.

Based on the results obtained through the loading plot (Fig. 6.15), significant factors whose average VIP score is ≥ 1 were identified using the VIP method. The VIP scores reflect the degree of importance with respect to X and Y variables. The average of squared VIP scores is equal to 1 when the VIP scores are equalized. The VIP plot displays the order of importance representing an intergroup priority ranking when the groups are classified. In the samples collected from Wonju

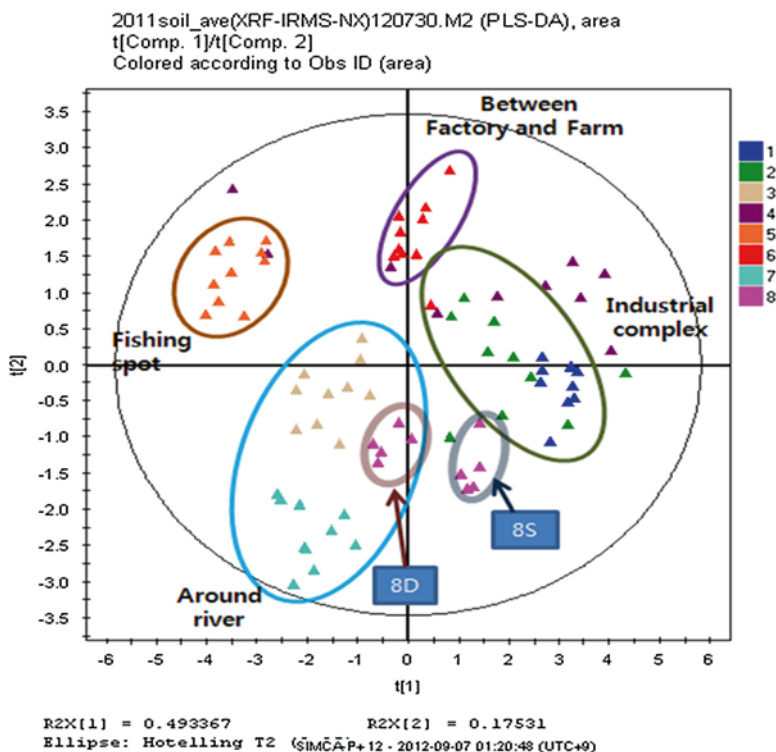


Fig. 6.14 PLS-DA score plot(*S*: on the surface, *D*: from a depth of 30 cm)

(Gangwondo, South Korea), the factors whose average VIP score was ≥ 1 were identified as SiO_2 , Fe_2O_3 , TiO_2 , and a* color factor (see Fig. 6.16 and Table 6.5).

In the factors whose average VIP score is ≥ 1 , the top four factors are shown on the loading plot (Fig. 6.10). As shown on the loading plot, they are distributed along the far ends of the quadrants divided by the y axis.

Comparison of the Statistical Analysis Results: SPSS Multivariate Analysis vs. Simca PLS-DA

A stepwise selection method was used in the SPSS discriminant analysis, where the significance tests using Wilks' lambda and exact F statistics on the variables entering in each step confirmed the entering order of CaO and TiO_2 . In the SIMCA loading plot, K_2O and CaO are on extreme edge of the 2nd and 4th quadrant, respectively.

According to standardized canonical-discriminant-function coefficients that furnish the explanatory power of discriminant functions, Function 1 exhibited a high explanatory power for the components SiO_2 (Fe_2O_3 , TiO_2), and discriminant Function 2 exhibited a high explanatory power for color factors B* ($\delta^{13}\text{C}$, carbon content).

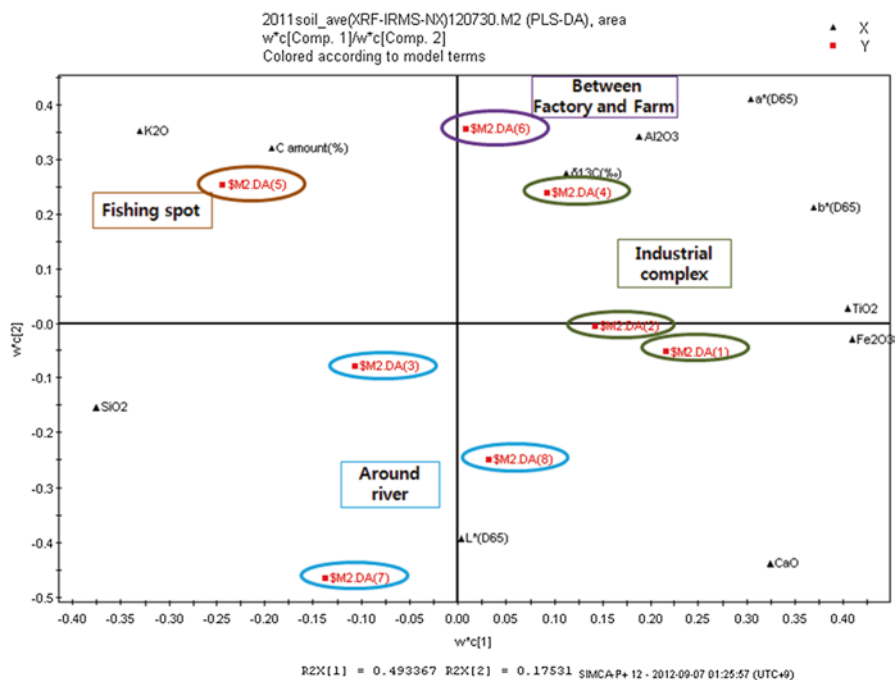


Fig. 6.15 Loading plot

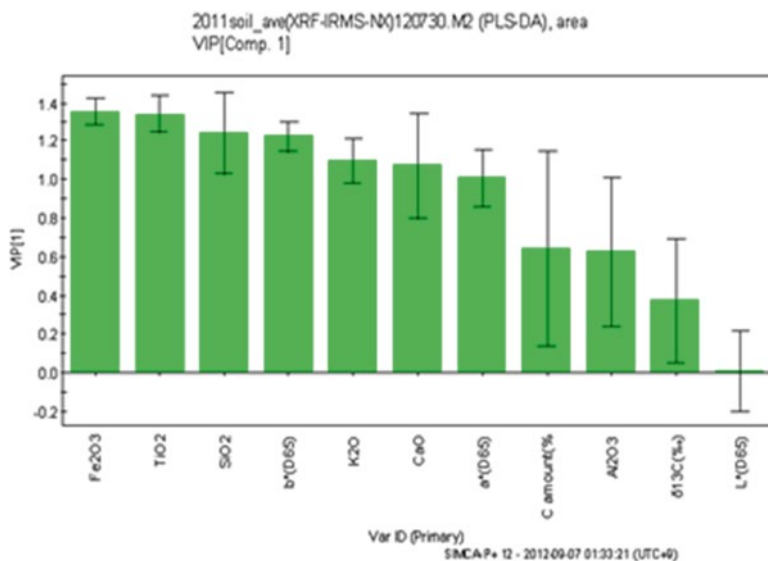


Fig. 6.16 VIP plot

Table 6.5 Determinant factors (VIP ≥ 1)

Var ID (Primary)	M2.VIP[1]	1.89456 * M2.VIP[1] cvSE
Fe2O3	1.35649	0.0661687
TiO2	1.34238	0.100236
SiO2	1.24434	0.213469
b*(D65)	1.22531	0.0779343
K2O	1.09671	0.11571
CaO	1.0738	0.273555
a*(D65)	1.00653	0.147745
C amount (%)	0.63997	0.505365
Al2O3	0.624347	0.382421
$\delta^{13}C(\text{‰})$	0.373935	0.319269
L*(D65)	0.00906133	0.205676

$\delta^{13}C$ and carbon content can be considered as the factors with a high explanatory power whereas their SIMCA VIP scores are lower than 1. From this result, it may be inferred that these factors are dependent more on depth rather than area.

Discriminant Analysis

A discriminant analysis that was performed using all the data obtained (color, XRF, IRMS) confirmed 100 % discriminating power.

In Box's M test, which was conducted to test the homogeneity of the between-group covariance matrices of 11 independent variables, homogeneity in between-group covariance matrices was not observed, individual-group covariance matrices were utilized when applying the classification method.

The discriminant analysis was performed using a stepwise method for selecting variables, where the significance of the variables entering in each step was tested using Wilks' lambda and exact F statistics. The results of the significance tests are listed in Table 6.6. The order of entrance was CaO and TiO₂.

Canonical correlation (CANCOR) reflects the degree of association between a discriminant function and a set of variables. The closer it is to 1, the higher is the discriminating power of the function. The correlation coefficients of Functions 1 and 2 obtained in this study are 0.975 and 0.961, respectively, which can be considered as excellent results. Moreover, a higher eigenvalue signifies a proportionally higher discriminating ability of a function. A function is then considered to have an excellent discriminating power.

Out of the two canonical discriminant functions obtained in the discriminant analysis in this study (Table 6.7), the eigenvalue of Function 1 was 19.625, which accounted for 49.1 % of the total discriminating power, and the discriminating power acquired by adding functions 2–7 to that of Function 1 was 100 %.

Table 6.6 Results of the significance tests using Wilk's lambda statistics and exact F statistics

Step	Entered	Wilks' Lambda											
		Exact F					Approximate F						
		Statistic	df1	df2	df3	Statistic	df1	df2	Sig.	Statistic	df1	df2	Sig.
1	CaO	.134	1	7	72.00	66.300	7.00	72.00	.00				
2	TiO ₂	.024	2	7	72.00	55.512	14.00	142.00	.00				
3	a*(D65)	.008	3	7	72.00					40.99	21.00	201.55	.00
4	b*(D65)	.003	4	7	72.00					34.71	28.00	250.21	.00
5	C amount (%)	.001	5	7	72.00					32.94	35.00	288.48	.00
6	δ ¹³ C	.000	6	7	72.00					31.94	42.00	317.71	.00
7	L*(D65)	.000	7	7	72.00					27.99	49.00	339.49	.00
8	Fe ₂ O ₃	.000	8	7	72.00					24.96	56.00	355.35	.00
9	SiO ₂	.000	9	7	72.00					23.27	63.00	366.56	.00
10	K ₂ O	.000	10	7	72.00					22.06	70.00	374.17	.00

At each step, the variable that minimizes the overall Wilks' Lambda is entered

^aMaximum number of steps is 22

^bMinimum partial F to enter is 3.84

^cMaximum partial F to remove is 2.71

^dF level, tolerance, or VIN insufficient for further computation

Table 6.7 Canonical correlation (CANCOR) of the discriminant functions

Function	Eigenvalue	% of variance	Cumulative %	CANCOR
1	19.625 ^a	49.1	49.1	.975
2	12.045 ^a	30.1	79.2	.961
3	4.481 ^a	11.2	90.4	.904
4	2.674 ^a	6.7	97.1	.853
5	.633 ^a	1.6	98.7	.623
6	.484 ^a	1.2	99.9	.571
7	.051 ^a	.1	100.0	.220

^aFirst seven canonical discriminant functions were used in the analysis

Table 6.8 Significance probability of discriminant functions

Test of function(s)	Wilks' Lambda	Chi-square	df	Sig.
1 through 7	.000	667.218	70	.000
2 through 7	.001	455.361	54	.000
3 through 7	.020	275.572	40	.000
4 through 7	.107	156.485	28	.000
5 through 7	.393	65.387	18	.000
6 through 7	.642	31.069	10	.001
7	.952	3.460	4	.484

As shown in Table 6.8, the significance probability of both Wilks' lambda value and Chi-square statistic for these discriminant functions is 0.000, which proves their significance. The only function that cannot be considered significant is Function 7 (0.484). Because Wilks' lambda tests the average homogeneity between the groups, its null hypothesis is "H0: i.e., there is no difference in the average between the groups." As the Wilks' lambda value decreases, the explanatory power of the corresponding function increases. Moreover, the significance probability of $\chi^2=667.218$ being 0.000 (<0.005), the null hypothesis is discarded and the discriminant function proves to be significant.

A standardized canonical discriminant function coefficient furnishes the explanatory power of a discriminant function; Function 1 has a high explanatory power for elements SiO₂ (Fe₂O₃, TiO₂), and Function 2 for color factors B* ($\delta^{13}\text{C}$, carbon content); see Table 6.9.

Table 6.10 lists the unstandardized canonical discriminant function coefficients. The discriminant score of each individual item was obtained by multiplying the value of each independent variable by the coefficient and subsequently adding the whole. The calculation modules of discriminant functions 1 and 2 are as follows:

$$D1 = -44.260 + 0.675\text{SiO}_2 + 0.893\text{Fe}_2\text{O}_3 - 1.303\text{K}_2\text{O} + 1.385\text{CaO} - 8.031\text{TiO}_2 - 0.452\delta^{13}\text{C} - 0.298\text{C amount} + 0.294\text{L}^* - 0.479\text{a}^*(\text{D65}) - 0.768\text{b}^*(\text{D65})$$

Table 6.9 The standardized canonical discriminant function coefficients of functions 1–7

Variables	Function						
	1	2	3	4	5	6	7
SiO ₂	1.733	.382	.048	.964	-.469	.032	-.098
Fe ₂ O ₃	1.360	-.194	.720	.194	.179	2.797	-.249
K ₂ O	-.848	-.709	.218	-.967	1.040	.375	.601
CaO	.783	.806	.918	-.713	.500	-.555	.347
TiO ₂	-1.103	-.066	-1.822	.139	-.108	-1.335	.467
δ13C	-.508	1.067	.122	.292	.103	.078	-.736
Carbon conc. (%)	-.196	1.116	.862	1.008	.492	.357	.966
L*(D65)	.507	-.046	.476	.627	-.361	.764	.550
a*(D65)	-.271	-.210	2.688	-.515	-1.035	-.741	-.033
b*(D65)	-.894	1.284	-1.988	.758	.747	.303	.324

Table 6.10 The unstandardized canonical discriminant function coefficients of functions 1–7

Variables	Function						
	1	2	3	4	5	6	7
SiO ₂	.675	.149	.019	.375	-.182	.013	-.038
Fe ₂ O ₃	.893	-.128	.473	.128	.117	1.838	-.163
K ₂ O	-1.303	-1.090	.335	-1.487	1.598	.576	.923
CaO	1.385	1.426	1.624	-1.261	.883	-.982	.613
TiO ₂	-8.031	-.481	-13.262	1.011	-.789	-9.719	3.398
δ13C	-.452	.950	.109	.260	.092	.069	-.655
C amount (%)	-.298	1.698	1.312	1.533	.748	.544	1.470
L*(D65)	.294	-.027	.276	.364	-.210	.443	.319
a*(D65)	-.479	-.371	4.747	-.909	-1.829	-1.309	-.058
b*(D65)	-.768	1.103	-1.709	.651	.642	.261	.278
(Constant)	-44.260	.122	-5.417	-32.157	8.310	-24.585	-46.649

$$D2 = 0.122 + 0.149\text{SiO}_2 - 0.128\text{Fe}_2\text{O}_3 - 1.090\text{K}_2\text{O} + 1.426\text{CaO} - 0.481\text{TiO}_2 \\ + 0.950\delta^{13}\text{C} + 1.698\text{C amount} - 0.027L^* - 0.371a^*(\text{D65}) + 1.103b^*(\text{D65})$$

Table 6.11 lists the discriminant scores produced by replacing independent variables with their means. The group centroids thus acquired indicate that Function 1 has a high discriminating power for Area 1, 3, 7, 8, and 6 than the other areas, and Function 1 has a high discriminating ability for Area 2, 4, and 5.

The classification using the canonical discriminant functions (D1 and D2) resulted in 100.0% discriminating accuracy for all the eight areas.

Table 6.11 Unstandardized canonical discriminant functions evaluated at group means

Area	Function						
	1	2	3	4	5	6	7
1	.256	1.118	.652	-3.581	-.747	-.442	-.029
2	-.183	6.046	-1.017	.482	1.018	-.457	-.211
3	1.873	-1.350	-.247	.549	.455	-.839	.454
4	-3.259	3.679	2.946	1.256	-.651	.684	.154
5	-1.152	-5.009	3.075	.014	.857	-.048	-.210
6	-7.966	-2.558	-2.944	.607	-.486	-.083	-.057
7	7.200	-1.155	-.562	1.700	-1.017	-.181	-.187
8	3.231	-.772	-1.903	-1.028	.570	1.365	.086

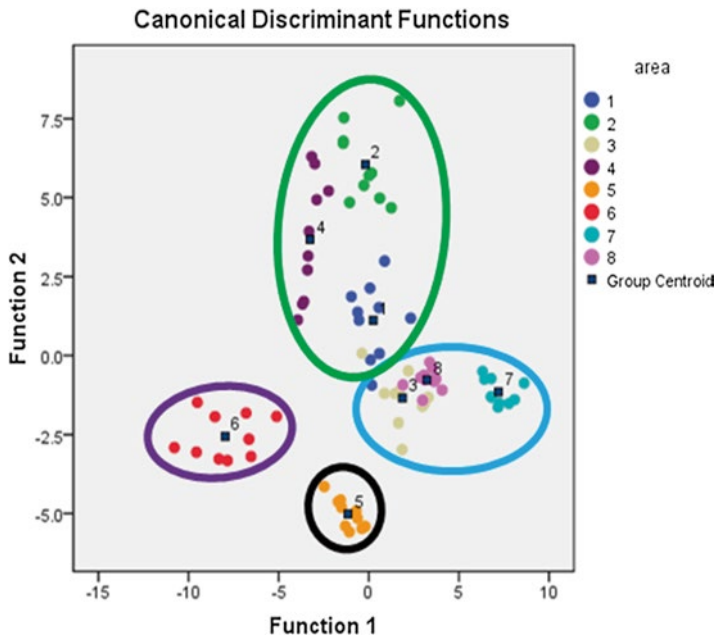


Fig. 6.17 Scatter plot displaying the discriminant scores

Figure 6.17 shows a scatter plot displaying the discriminant scores of the classification of all sub-samples performed by applying D1 and D2. Area 6 and 7 are well discriminated from other areas with D1 (horizontal axis), and Area 2 and 5 are well discriminated from other areas with D2 (vertical axis). A clustering tendency is observed according to area-specific characteristics: Area 3, 7, and 8 are located near the water, Area 1 and 2 near the industrial complex, Area 6 near the pasturing area and factories, and Area 5 in the fishing zone near the dam.

6.4 Conclusions

As a preliminary experiment to test the discriminating power of forensic soil analysis and obtain area-specific information, the soil analyses with respect to color, elements, and carbon-isotope ratio were performed. The results of analyses of the soil samples collected from the eight areas located in Munmak-eup (Wonju, Gangwondo, South Korea) are as follows.

1. The discriminating power regarding color, elements, and carbon content and isotope ratio was improved when all the three factors were combined compared to the discriminating power by individual data. In particular, the discriminating power for color and elemental analyses was excellent, and the results regarding carbon content and isotope ratio showed significant differences depending on soil depth.
2. The paired *t*-test on the results of carbon content and carbon isotope ratio measurements of the S and D samples confirmed that the samples had significant depth-dependent differences in carbon content.
3. The results of SIMCA PLS-DA performed on the samples collected from the eight areas in Wonju (Gangwondo, South Korea) showed that the Fe_2O_3 , TiO_2 , SiO_2 , and a^* color factors had an average VIP score greater than 1.
4. From the ANOVA tests, the null hypotheses for all the factors were rejected except that for Al_2O_3 .
5. The canonical-discriminant analysis on three soil characteristics (color, composition, and content) showed that Function 1 exhibited a greater explanatory power for SiO_2 (Fe_2O_3 , TiO_2), and could differentiate Area 6 and 7 more easily than the other areas. Function 2 had greater implications for color factor b^* ($\delta^{13}\text{C}$ and C content), and could differentiate Area 2 and 5 more efficiently. However, different results were obtained even within the same area, depending on the soil depth. Area 7 near the river, mainly formed with alluviums, has a high SiO_2 content and a relatively low Fe_2O_3 content.
6. During the elemental analysis, Al_2O_3 was categorized as an element without discriminating power owing to its extremely high RSD within the sub-sample. However, this may be attributed to the suppressed separation in the Br and XRF phase during the process of bead production. Therefore, in the case Al analysis using XRF, the beads should be made without using the remover, or pellets should be made instead of beads. If the remover is added, the sample should be analyzed with other methods such as LA-ICP-MS or ICP-AES.
7. Future studies should be performed for the analysis of Zn, Cu, and platinum group elements (PGE) (Pt, Pd, and Rh) in order to obtain the vehicle-related information. Further, Zn, Cu, Pb, Sn, and Ag elements should be analyzed. The nitrogen-related tests should be reconsidered, given its ability to discriminate the soil's origin in water environment.
8. In order to obtain more useful information, the results obtained in this study should be compared with those performed on samples collected from the areas at some distance from the experimental areas. Furthermore, by performing experiments in other regions, a more concrete and systematic region-specific information can be established.

References

- Bull PA, Parker A, Morgan RM (2006) The forensic analysis of soil and sediment taken from the cast of a footprint. *Forensic Sci Int* 162:6–12
- Chaperlin K, Howarth PS (1983) Soil comparison by the density gradient method – a review and evaluation. *Forensic Sci Int* 23:161–177
- Cox RJ, Peterson HL, Young J, Cusik C, Espinoza EO (2000) Forensic analysis of soil organic by FTIR. *Forensic Sci Int* 108:107–116
- Fitton G (1997) X-ray fluorescence spectrometry. In: Gill R (ed) *Modern analytical geochemistry: an introduction to quantitative chemical analysis techniques for earth, environmental and materials scientists*. Addison Wesley Longman, London, pp 87–115
- Graves WJ (1979) A mineralogical soil classification technique for the forensic scientist. *J Forensic Sci* 24:323–338
- Guedes A, Ribeiro H, Valentim B, Rodrigues A, Sant’Ovaia H, Abreu I, Noronha F (2011) Characterization of soils from the Algarve region (Portugal): a multidisciplinary approach for forensic applications. *Sci Justice* 51:77–82
- Junger EP (1996) Assessing the unique characteristics of close-proximity soil samples: just how useful is soil evidence? *J Forensic Sci* 41:27–34
- Kim K (2007) Metabolic profiling of hair from patients with skin appendage diseases by gaschromatography-mass spectrometry, Yonsei University
- Meyers PA (1994) Preservation of elemental and isotopic source identification of sedimentary organic matter. *Chem Geol* 114:289–302
- Murray RC (2012) Forensic examination of soils. In: Kobilinsky L (ed) *Forensic chemistry handbook*. Wiley, Hoboken
- Park HH, Ok CS, Kang SS, Ko SJ, Choi SY (2011) Recognition for lung cancer using PCA in the digital chest radiography. *J Korean Inst Inf Commun Eng* 15(7):1573–1582
- Petraco N, Kubic T (2000) A density gradient technique for use in forensic soil analysis. *J Forensic Sci* 45(4):872–873
- Petraco N, Kubic TA, Petraco NDK (2008) Case studies in forensic soil examinations. *Forensic Sci Int* 178(2):e23–e27
- Pye K, Blott SJ (2009) Development of a searchable major and trace element database for use in forensic soil comparisons. *Sci Justice* 49:170–181
- Pye K, Blott SJ, Croft DJ, Carter JF (2006) Forensic comparison of soil samples: assessment of small-scale spatial variability in elemental composition, carbon and nitrogen isotope ratios, colour, and particle size distribution. *Forensic Sci Int* 163:59–80
- Pye K, Blott SJ, Croft DJ, Witton SJ (2007) Discrimination between sediment and soil samples for forensic purposes using elemental data: an investigation of particle size effects. *Forensic Sci Int* 167:30–42
- Reuland DJ, Trinler WA (1981) An investigation of the potential of high performance liquid chromatography for the comparison of soil samples. *Forensic Sci Int* 18:201–208
- Thanasoulis NC, Piliouris ET, Kotti M-SE, Evmiridis NP (2002) Application of multivariate chemometrics in forensic soil discrimination based on the UV–vis spectrum of the acid fraction of humus. *Forensic Sci Int* 130:73–82
- Wheals BB, Noble W (1972) Forensic applications of pyrolysis gas chromatography. *Chromatography* 5(9):553–557